A HISTOPATHOLOGICAL SURVEY WITH A FOCUS ON HEPATOPANCREAS AND GUT OF FARMED PACIFIC WHITE SHRIMP *(PENAEUS (L) VANNAMEI)*

Dissertation submitted in partial fulfillment
of the requirements
for the degree of

M.F.Sc. (Aquatic Animal Health Management)

By

M. ARUL MURUGAN, B.F.Sc.

(AAHM-MA6-01)

ICAR-CENTRAL INSTITUTE OF FISHERIES EDUCATION

(University Established Under Section 3 of UGC Act 1956)

**Panch Marg, Off Yari Road, Versova, Andheri (W),
Mumbai – 400 061**

JUNE, 2018

M. Arul Murugan, 2018. A histopathological survey with a focus on hepatopancreas and gut of farmed pacific white shrimp *(Penaeus (L) vannamei)*. M.F.Sc. Dissertation, ICAR-Central Institute Of Fisheries Education (University Established Under Section 3 of UGC Act 1956), Panch Marg, Off Yari Road, Versova, Andheri (W), Mumbai – 400 061

Dedicated to

My Family & Friends

भा.कृ.अ.प. - केन्द्रीय मात्स्यिकी शिक्षा संस्थान
ICAR-CENTRAL INSTITUTE OF FISHERIES EDUCATION
(A university Established Under Sec.3 of UGC Act 1956)
Ministry of Agriculture, Govt. of India

Dated : 30th June, 2018

CERTIFICATE

Certified that the dissertation entitled **"A HISTOPATHOLOGICAL SURVEY WITH A FOCUS ON HEPATOPANCREAS AND GUT OF FARMED PACIFIC WHITE SHRIMP (*PENAEUS (L) VANNAMEI*)"** is a bonafide record of independent research work carried out by **Mr. M. Arul Murugan** during the period of study from August, 2017 to June, 2018 under our supervision and guidance for the degree of **Master of Fisheries Science (Aquatic Animal Health Management)** and that the dissertation has not previously formed the basis for the award of any degree, diploma, associateship, fellowship or any other similar title.

Advisory Committee

Major Advisor

(K.V. Rajendran)
Principal Scientist & Head
Aquatic Environment & Health Management Division
CIFE, Mumbai-61

(Megha K. Bedekar)
Senior Scientist
Aquatic Environment &
Health Management Division
ICAR-CIFE, Mumbai-61

(Sanath Kumar H)
Senior Scientist
Fisheries Resources, Harvest &
Post-Harvest Management Division
ICAR-CIFE, Mumbai-61

(Sreedharan K)
Scientist
ICAR-CIFE Rohtak Centre
Rohtak-11

पंच मार्ग, ऑफ यारी रोड, वरसोवा, अंधेरी (प.), मुंबई - ४०० ०६१. (भारत)
Panch Marg, Off Yari Road, Versova, Andheri (W), Mumbai - 400 061. (India)
कार्यालय / Office) : 022-26361446/7/8,
Fax : 022-26361573
Website : http ://cife.edu.in

सर्व शिक्षा अभियान
सब पढ़ें सब बढ़ें

DECLARATION

I hereby declare that the dissertation entitled "**A HISTOPATHOLOGICAL SURVEY WITH A FOCUS ON HEPATOPANCREAS AND GUT OF FARMED PACIFIC WHITE SHRIMP (*Penaeus (L) vannamei*)**" is an authentic record of the work done by me and that no part thereof has been presented for the award of any degree, diploma, associateship, fellowship or any other similar title.

Date: 30 June, 2018 **M. ARUL MURUGAN**

Place: Mumbai M.F.Sc Student

ICAR- Central Institute of Fisheries Education

ACKNOWLEDGEMENT

This dissertation would not have been possible without the guidance and the help of several individuals who in one way or another contributed and extended their valuable assistance in the preparation and completion of this study. While few names are being mentioned many more are missing, but I hope those names shall be read between the lines, I owe deep seated gratitude to all those missing names.

First and foremost, I thank Almighty who is benevolent, beneficent and whose blessings have solely contributed for my success during my dissertation and till this phase of life.

It is a great privilege as well as pleasure to express my sincere and deepest sense of gratitude to my advisor ***Dr. K.V. Rajendran.,*** *Principal Scientist & Head, Aquatic Environment and Health Management Division, CIFE, Mumbai for his continuous support, constant supervision, patience, understanding, motivation, timely decisions, focus, simplicity, guidance and immense knowledge. His guidance helped me in the time of research and writing of this dissertation. I could not have imagined having a better advisor and mentor for my M.F.Sc programme. Thank u sir, for making me feel special as I got a guide like u.*

I whole heartedly thank my Co-advisor ***Dr. Sreedharan Krishnan,*** *Scientist, Aquatic Environment and Health Management Division, CIFE, Rohtak centre, for his continuous support, genuine interest, ideas, suggestions, constant encouragement and loving care throughout my research process.*

I would like to thank my advisory member ***Dr. Sanathkumar H,*** *Senior Scientist, FRHPHM Division, CIFE, Mumbai for his help during this study. Thank you so much Sir for your guidance. I would also like to thank my advisory member* ***Dr. Megha Kadam Bedekar****, Senior Scientist, AEHM Division, CIFE, Mumbai for her help during my research work.*

It is my honor and great privilege to express my deep sense of gratitude to ***Dr. Gopal Krishna****, Director, ICAR-CIFE for providing the necessary facilities needed for conducting the study.*

Words would not be enough to thank and express my gratitude to ever memorable ***Dr. Amod Kulkarni*** *for his untiring support, love, care, guidance, encouragement and imbibing positive thoughts during the time of necessity in my entire research work. Thank you very much Sir, for being a Guru. I have nothing to repay you sir other than keeping the memories I had with you.*

I offer my heartiest gratitude and thankfulness to ***Aathish bhai*** *who has been a great helping hand in my research work. I thank him for being a friend and I will always be grateful for the help he rendered during my research work. A*

*special thanks to **Deepika mam** for her timely support and technical help besides her busy routine. I am very much thankful to all faculty and staff of Department of Aquatic Animal Health Management for their support throughout my research work.*

*I shall ever remain indebted to my ever loving friends **Safna, Sathya, Akash, Dhaya, Vandhana, Bharathi, Pushpa, Ramesh,** and **Vismai** for being with me all the time of my happiness and worries. I will always cherish the memories I had with you all.*

*My hearty and genuine thanks to my beloved seniors, **Rahul sir Santhanam sir, Kantharajan sir, Srihari sir** and **Abu sir** for their timely suggestions and valuable contribution to my research work.*

*My special thanks to **Nalini Poojary mam, Gayathri** and **Akeeth** for rendering help to work in laboratory.*

*I sincerely acknowledge the **ICAR** and **CIFE** for providing me fellowship throughout the study period.*

Most importantly, I owe my loving thanks to my Mother, Brother and Grandma for supporting me spiritually throughout this period. Without their encouragement, prayers and understanding it would have been impossible for me to conduct this study. A special thanks to my family for having belief in me and sending me to CIFE for higher studies.

Finally, for those of you, whose names I could not mention here, I offer my apologies but know that you have made this experience so special that will never be forgotten.

Place: Mumbai

Date: 30.06.2018 ***(M. Arul Murugan)***

सारांश

हिस्टोपैथोलॉजी सबसे बहुमुखी उपकरण में से एक है जिसका उपयोग बीमारी का निदान करने के साथ-साथ रोग प्रक्रिया / स्थिति को विशेष रूप से झींगा में समझने के लिए किया जा सकता है। झींगा रोगों में से कई को सामान्य हिस्टोलॉजिकल आर्किटेक्चर और हेपेटोपैंक्रियास के कामकाज को प्रभावित करने और बीमारी की स्थिति के कारण आंत को प्रभावित करने की सूचना मिली है। वर्तमान अध्ययन में, हेपेटोपैनक्रियास और कुल 60 खेती चिंराट, पेनेउस (लिटोपनेयस) वनामेई से दो अलग-अलग कृषि प्रणालियों जैसे हेन्डल लवण जलीय कृषि (हरियाणा) और ब्रैकिशवॉटर जलीय कृषि (महाराष्ट्र) से हिटोपोलिकक्रिया और आंत का विश्लेषण किया गया। महाराष्ट्र से एकत्रित झींगा में पाए गए मंद विकास को छोड़कर, कोई सकल पैथोलॉजिकल परिवर्तन नहीं, अध्ययन के दौरान एकत्रित झींगा में मनाया गया था। अध्ययन के दौरान एकत्रित पचास जानवरों को भी रोगी / बीमारियों जैसे ईएचपी, डब्लूएसएसवी, आईएचएनएनवी, एचपीवी, एमबीवी, एएचपीएनडी और एनएचपी के लिए परीक्षण किया गया था। हेपेटोपैंक्रियास में मध्यम से गंभीर हिस्टोपैथोलॉजिकल बदलावों को देखा गया था और इनमें ट्यूबलर नेक्रोसिस, डिटेचमेंट और ट्यूबलर एपिथेलियम, ट्यूबलर एट्रोफी, भारी हेमोसाइटिक घुसपैठ, असामान्य रूप से बढ़ी हुई हेमल साइनस, इंकापुलेशन, नोड्यूल गठन और मेलानिज़ेशन शामिल है। हेपेटोपैंक्रियास ने एंटरोसाइटोज़ून हेपेटोपेनेई (ईएचपी) की उपस्थिति को गहराई से बेसोफिलिक समावेशन के रूप में भी प्रकट किया- जैसे प्लसोडिया ट्यूबल साइटप्लाज्म में वैक्यूल्स और नेक्रोटिज्ड लुमेन में बीजों के एकत्रीकरण के भीतर निहित है। माइक्रोस्कोपीडियन द्वारा प्रेरित नेक्रोसिस के विभिन्न चरणों की भी पहचान की गई। पीसीआर स्क्रीनिंग ने अंतर्देशीय खारे पानी (20%) की तुलना में ब्रैकिशवॉटर सिस्टम में खेती गई चिंराट में ईएचपी (60%) के उच्च प्रसार का खुलासा किया। दिलचस्प बात यह है कि हेपेटोपैंक्रेटिक ट्यूबल के स्लोउड लुमेन में समेकित माइक्रोविलि (एटीएम) जैसी निकायों को भी देखा गया। हालांकि, संस्कृति तालाबों में कोई सफेद फिकल स्ट्रैंड दर्ज नहीं किया गया था। तीव्र हेपेटोपैंक्रेटिक नेक्रोसिस बीमारी (एएचपीएनडी)-जैसी पैथोलॉजी असामान्य रूप से बढ़ी हुई हेमल साइनस और दूर-दराज, मध्यवर्ती और हेपेटोपैंक्रियास के समीपवर्ती भाग में नेक्रोटिज्ड ट्यूबल के मेलेनोसिस द्वारा चिह्नित किया गया था। हालांकि, पीसीआर विश्लेषण ने एएचपीएनडी संक्रमण प्रकट नहीं किया। फिर भी, हेपेटोपैंक्रेटिक लुमेन में रॉड के आकार वाले जीवाणुओं की उपनिवेशों को देखा गया। कुछ झींगा के हेपेटोपैंक्रियास में नेक्रोटिंग हेपेटोपैंक्राइटिस (एनएचपी) जैसा ही हिस्टोपैथोलॉजी भी देखा गया था। इसमें लुमेन का विस्तार और उपकला परत का पूर्ण अपघटन शामिल था, लेकिन हेमोकैटिक घुसपैठ और हेमल साइनस के विस्तार के बिना। हालांकि, पीसीआर विश्लेषण ने एनएचपी बैक्टीरिया के किसी भी प्रवर्धन को नहीं दिखाया। कुछ जानवरों में ईएचपी और बैक्टीरिया के साथ सह-संक्रमण भी देखा गया था जिसमें नेत्रोटिज्ड हेपेटोपैनक्रियास ने ईएचपी स्पायर्स और जीवाणु कॉलोनी का खुलासा किया था। जानवरों के आंत हिस्टोलॉजी ने अधिकांश मामलों में कोई महत्वपूर्ण रोगविज्ञान नहीं दिखाया। हालांकि, झींगा में आंत उपकला का भारी अपघटन देखा गया था, जिसमें हेपेटोपैनक्रियास में गंभीर रोगविज्ञान दिखाई देता था। पीसीआर विश्लेषण ने वर्तमान अध्ययन के दौरान परीक्षण किए गए किसी भी वायरस के लिए सकारात्मक प्रवर्धन नहीं दिखाया। वर्तमान अध्ययन से खेती हुई चिंराट के हेपेटोपैंक्रियास में गंभीर हिस्टोपैथोलॉजिकल परिवर्तनों की उपस्थिति से पता चला है जो अंग के असफलता और जलीय कृषि में परिणामी पुरानी बीमारी की स्थिति का कारण बन सकता है।

Abstract

Histopathology is one of the most versatile tools which can be used in diagnosing the disease as well as to understand disease process/condition especially in shrimp. Many of the shrimp diseases have been reported to affect the normal histological architecture and functioning of the hepatopancreas and gut leading to disease conditions. In the present study, hepatopancreas and gut from a total of 60 farmed shrimp, *Penaeus* (*Litopenaeus*) *vannamei* from two different farming systems viz., inland saline aquaculture (Haryana) and brackishwater aquaculture (Maharashtra) were analysed histologically. No gross pathological changes, except for the retarded growth found in shrimp collected from Maharashtra, were observed in shrimp collected during the study. Forty-five animals collected during the study were also tested for pathogens/diseases such as EHP, WSSV, IHHNV, HPV, MBV, AHPND and NHP. Moderate to severe histopathological alterations were observed in the hepatopancreas and these included tubular necrosis, detachment and complete sloughing of tubular epithelium, tubular atrophy, heavy haemocytic infiltration, abnormally enlarged haemal sinuses, encapsulation, nodule formation and melanisation. The hepatopancreas also revealed the presence of *Enterocytozoon hepatopenaei* (EHP) as deeply basophilic inclusion-like plasmodia contained within the vacuoles in tubule cytoplasm and aggregations of spores in the necrotized lumen. Different stages of necrosis induced by the microsporidian were also identified. PCR screening revealed higher prevalence of EHP (60%), in shrimp farmed in brackishwater system compared to the inland saline water (20%). Interestingly, aggregated transformed microvilli (ATM)-like bodies were also observed in the sloughed lumen of hepatopancreatic tubules. However, no white faecal strands were recorded in the culture ponds. Acute hepatopancreatic necrosis disease (AHPND)-like pathology marked by abnormally enlarged haemal sinuses and melanosis of necrotized tubules in the distal, medial as well as proximal part of hepatopancreas was also observed. However, PCR analysis did not reveal AHPND infection. Nevertheless, colonies of rod-shaped bacteria were observed in the hepatopancreatic lumen. Histopathology resembling necrotising hepatopancreatitis (NHP) was also observed in the hepatopancreas of some of the shrimp. This included enlargement of lumen and complete degeneration of epithelial layer but without haemocytic infiltration and enlargement of haemal sinuses. However, PCR analysis did not show any amplification of NHP bacterium. Co-infection with EHP and bacteria was also noticed in some of the animals in which necrotised hepatopancreas revealed EHP spores and bacterial colony. Gut histology of the animals did not show any significant pathology in majority of cases. However, heavy degeneration of gut epithelium was noticed in shrimp which showed severe pathology in the hepatopancreas. PCR analysis did not show positive amplification for any of the viruses tested during the present study. The present study revealed the presence of severe histopathological changes in the hepatopancreas of farmed shrimp which might lead to the dysfunction of the organ and resultant chronic disease conditions in aquaculture.

CONTENTS

LIST OF TABLES

LIST OF FIGURES

LIST OF PLATES

INTRODUCTION

1. INTRODUCTION

Aquaculture is one of the fastest growing food-production sectors in the world, which provides employment, income and livelihood support to many people in the world. Shrimp farming in India is a highly profitable business garnering huge returns in billions of dollars through exports. Indian shrimps have acquired an established position in the global market and is being exported to around 80 countries in the world (www.exportgenius.in). Presently, Indian shrimp aquaculture industry is dominated by Pacific white shrimp, *Penaeus (Litopenaeus) vannamei* (Boone, 1931), the exotic penaeid shrimp, which has become the most important export commodity, replacing the indigenous *Penaeus monodon (P. monodon)* from the Indian aquaculture scenario. According to the production statistics from Marine Products Export Development Authority, export production of *Penaeus vannamei (P. vannamei)* contributed up to 406,018 mt in 2015–16 utilizing 59,116 ha area in India. The export of *P. vannamei* has contributed immensely to the Indian seafood export, contributing 70% by value (MPEDA, 2015).

Presently, diseases caused by various agents have affected the sustainability of shrimp industry in many countries of the world. The major cause of increased incidences of diseases have been attributed to modernization of culture techniques such as increased stocking densities and use of pelleted feeds, which results in deterioration and imbalance in aquatic environment leading to diseases of varying nature (Alavandi *et al.,* 1995). Major disease causing agents include viruses, bacteria, parasites, fungi, nutritional and environmental factors, and all these pose a major threat to the production of farmed shrimp. The potential shrimp viruses include white spot syndrome virus (WSSV), Taura syndrome virus (TSV), Yellow head virus (YHV), Covert mortality nodavirus (CMNV), Infectious myonecrosis virus (IMNV), Infectious hypodermal and haematopoietic necrosis virus (IHHNV), Hepatopancreatic parvovirus (HPV), Monodon baculovirus (MBV) etc. In recent years, early mortality syndrome (EMS) or acute hepatopancreatic necrosis disease (AHPND), caused by *Vibrio parahaemolyticus* VP_{AHPND} has emerged and rapidly

spread in Asian countries and Mexico (Tran *et al.,* 2013; Dong *et al*., 2017) and resulted in heavy economic losses to shrimp production. Moreover, the shrimp farms in the Southeast Asian countries have recently been affected by the microsporidian parasite, *Enterocytozoon hepatopenaei* (EHP) (Rajendran *et al*., 2016; Tang *et al*., 2016). Majority of these diseases lead to huge production loss in the shrimp culture industry worldwide either due to the growth retardation or mortality resulting from infectious microorganisms.

The deadly diseases caused by different pathogens affect the shrimp's vital organs differently (Lightner *et al*., 1983; Flegel., 1997; Tran *et al*., 2013; Rajendran *et al*., 2016); however, the target organ of the pathogens differs from each other. This makes monitoring the health status in shrimp difficult, hindering the early detection of diseases which is crucial for the effective health management of farmed animals. Majority of the shrimp diseases have been reported to affect the normal histological architecture and functioning of the hepatopancreas and gut, inflicting adverse effects on the health of the animal.

Hepatopancreas (HP) is a large bi-lobed glandular organ accounting for about 2 to 6% of total body weight of shrimp, and performs the functions of liver and pancreas (Manan *et al*., 2015). Generally, the shape and color of the HP can be used as an indicator of shrimp health condition and can also be used to identify the severity of problems that affect the animal (Manan *et al.,* 2015). Solid, triangular, brown colored HP is an indicator of healthy shrimp with optimum appetite. The healthy, solid hepatopancreas is composed of numerous blind ending tubules and the whole organ is enveloped by a layer of thin connective tissue called tunica propria. The tubules consists of a central lumen which in turn are lined with a layer of epithelium (Gibson and Parker, 1979). There are five types of cells in the tubule epithelium namely E- (embryonic or Embryozellen) cells, F- (fibrillar) cells, B- (blister-like or Blastozellen) cells (Jacobs, 1928), R- (resorptive/absorptive or Restzellen) cells and M- (midget) cells (Al-Mohanna *et al*., 1985), and four of them have been studied microscopically to describe the health condition of the shrimp (Bell and Lightner, 1988). Diseases namely, hepatopancreatic microsporidiosis caused by

EHP, early mortality syndrome (EMS or AHPND) by *Vibrio parahaemolyticus* $VP_{AHPND,}$ necrotizing hepatopancreatitis (NHP) caused by rickettsial-like organism are known to directly affect HP causing pathological changes. Viruses such as HPV and MBV also cause discernible histological changes in HP. Besides, many diseases of obscure etiology infecting *P. vannamei* worldwide such as slow/retarded growth, white feces syndrome (WFS)/white gut disease (WGD) are reported to cause pathological alterations in HP and lead to hepatopancreatic dysfunction. Further, diseases of non-infectious origin have also shown direct effect on the HP of many crustaceans including shrimps (Sreeram *et al*., 2005; Sousa and Petriella*,* 2007; Diaz *et al*., 2010).

Besides hepatopancreas, gastrointestinal tract which includes stomach (foregut), midgut and hindgut are also susceptible to pathogens. Stomach and hindgut are lined with cuticular layer which acts as a barrier to pathogens/antigens entering *per os*. On the other hand, midgut possesses epithelial layer which is covered by a peritrophic membrane (Soonthornchai *et al*., 2015). The midgut region being devoid of exoskeletal lining becomes an easy target for the penetrating pathogens which enter the alimentary canal along with the ingested water, food and sediments (Ruby *et al*., 1980, Jayabalan *et al*., 1982). Among the pathogens infecting digestive system of shrimp, bacterial pathogens belonging to the family Vibrionaceae, *V. harveyi* and *V. parahameolyticus* play a significant role, causing severe damage to the epithelial cells of midgut and the underlying basement membrane and complete destruction of the gut epithelium (Soonthornchai *et al.,* 2010). Among viruses, WSSV is known to cause severe pathology in shrimp gut, especially in the endothelial cells of the hindgut lining (Manjusha *et al*., 2009). Parasitic infections by EHP can also affect the midgut through formation of spores in the midgut epithelium (Tang *et al.,* 2016).

Histopathology is one of the most versatile tools which can be used in diagnosing the disease as well as to understand disease process/condition especially in shrimp. Histopathology has been used to diagnose most of the diseases infecting shrimp and in some cases it is used as the confirmatory test. The advantage

of histological techniques over molecular techniques like PCR is that it can be applied in identifying the disease condition when the etiology is obscure. Further, when used in conjunction with molecular tools, it can be one of the most potent tools to understand the health status of the animals. Against this background, it is convincing to hypothesise that studying the status and condition of hepatopancreas and gut in farmed shrimp will provide significant evidences in assessing the health status of the animal. Although information is available on the normal and pathological conditions of hepatopancreas and gut of shrimps, a histological survey is warranted to explore the health status of farmed *P. vannamei*, especially in the context of many emerging diseases of obscure etiology in farmed shrimp. Against this background, the proposed study is envisaged with the following objectives.

1. To study various histopathological changes in the hepatopancreas and gut of farmed shrimp, *Penaeus (L) vannamei*
2. To correlate the histopathological changes to identified etiological agents

REVIEW OF LITERATURE

2. REVIEW OF LITERATURE

Shrimps are susceptible to diverse types of pathogens including parasites, fungi, protozoa, rickettsiae, bacteria and viruses resulting in huge losses in aquaculture. Among the various organisms, viruses have been the most calamitous pathogens causing mass mortalities in shortest possible time. Among major pathogen encountered in shrimp aquaculture, only white spot syndrome virus (WSSV), infectious hypodermal and haematopoietic necrosis virus (IHHNV), hepatopancreatic parvovirus (HPV) and monodon baculovirus (MBV) target hepatopancreas for their replication and cause cellular changes. WSSV and IHHNV are reported to be infecting only the inter-tubular connectives of hepatopancreas. WSSV, IHHNV and MBV also infect gut epithelium of shrimp. The other viral pathogen which infects the shrimp gut is Taura syndrome virus (TSV). Besides the viruses, bacteria, parasites and many abiotic factors cause significant pathological conditions in hepatopancreas and gut of shrimp.

In order to identify the pathological/physiological changes, a thorough knowledge on normal cellular structures is mandatory. Accordingly, hepatopancreas has been a target tissue of study by different workers to describe the normal as well as pathological conditions. Morphology of the shrimp hepatopancreas has been described from early 20th century by Hirsch and Jacobs (1928). Bell and Lightner (1988) provided illustrative details of penaeid histology including the hepatopancreas. Morales *et al*. (1999) performed histopathological studies on wild broodstock of white shrimp *Penaeus vannamei* in the Platanitos area, Mexico, to study the prevalence and severity grade of the infectious diseases affecting *P. vannamei*.

2.1 Histopathological changes due to viral infections

Many viruses have been reported to cause histological changes in hepatopancreas of shrimp. Major viral diseases affecting the farmed shrimp in India include the diseases caused by WSSV, IHHNV, MBV, HPV and IMNV. In an earlier

study, Lightner *et al*. (1983) reported the IHHNV infection for the first time in *Litopenaeus stylirostris* and *P. vannamei* and the major histological observations revealed Cowdry type A inclusion bodies in the hypertrophic nuclei of cells of stomach epithelium. Later, Bell and Lightner (1984) showed the pathognomic eosinophilic Cowdry type A inclusion bodies in the foregut epithelium of *L. stylirostris* and *P. vannamei* experimentally infected with IHHNV. Owens *et al*. (1992) reported presence of IHHNV in a batch of *P. esculentus* hybridized with *P. monodon* in Australia and they noticed characteristic Cowdry type A inclusions in the connective tissue between the tubules of hepatopancreas. Lightner (1996) reported a preliminary diagnosis for IHHNV based on identifying the intranuclear, Cowdry type A inclusion bodies within the chromatin-marginated, hypertrophied nuclei. Singhapan *et al*. (2004) studied the effect of IHHNV on growth and survival of *P. vannamei* and observed the presence of eosinophilic intranuclear inclusion bodies in the intertubular connective tissues of hepatopancreas. Lightner (2011), in his review on the virus diseases of farmed shrimp in America showed that the characteristic IHHNV inclusion bodies are eosinophilic and often appear as haloed intranuclear inclusion bodies within chromatin-marginated, hypertrophied nuclei of cells in tissues of epithelium of foregut and hindgut. Pazir *et al*. (2012) studied the histopathology of IHHNV infection in *P. vannamei* and the major histological findings included widespread cellular degeneration, severe nuclear hypertrophy and margination of chromatin in the cells of gut epithelium and large intra nuclear eosinophilic Cowdry A type inclusions in the connective tissues of hepatopancreas.

Lightner (1996) reported the histological identification of WSSV and noticed the intranuclear inclusion bodies within the hypertrophied nucleus. Chang *et al*. (1996) noticed the susceptibility of the connective tissue and the myoepithelial cells of the connective sheath in hepatopancreas of *P. monodon* to WSSV, however, no inclusion bodies could be found in the tubules of the hepatopancreas. Tapay *et al*. (1997) noticed hypertrophied nuclei in the foregut epidermis and the subepidermal connective tissue beneath the stomach epithelium in experimentally infected *P. vannamei* with WSSV. They also reported hepatopancreas to be refractive to WSSV infection. Lightner *et al*. (1998) studied the experimental infection

of *P. vannamei* with WSSV and histopathological features included the characteristic intranuclear eosinophilic to basophilic inclusion bodies in cells of the cuticular epidermis of the foregut and the hindgut of *P. vannamei*. Mohan *et al*. (1998) studied the histopathology of cultured shrimps showing gross signs of WSSV and the study revealed the hypertrophied nuclei with intranuclear inclusions in the subcuticular gut epithelium of *P. monodon* infected with WSSV. Wang *et al*. (1999) studied the histopathology of WSSV in *P. monodon* and the major histopathological changes observed were increased cellular vacuolization in the hepatopancreatic epithelial cells with reduction in the number of B-cells and the presence of intranuclear inclusions in the stomach wall. Histological study by Sudha *et al*. (1998) in *P. monodon* and *P. indicus* following WSSV infection revealed the basophilic intranuclear inclusion bodies in the hypertrophied nuclei of the foregut cuticular epithelium. Rajendran *et al*. (1999) studied the histopathology of experimentally infected crustaceans and their study showed the characteristic deeply stained, prominent intranuclear inclusions in the cuticular ectodermal layer of the gut. The study of Yoganandhan *et al*. (2003) revealed the cellular degeneration, severe nuclear hypertrophy with intranuclear inclusion bodies and chromatin margination in the stomach epithelium of *P. indicus* following WSSV infection. Rodriguez *et al*. (2003) studied the histopathology of natural infection with WSSV in *P. vannamei,* and they noticed severely infected stomach cuticular epithelium of *P. vannamei* showing nuclear hypertrophy with the presence of eosinophilic intranuclear inclusion bodies. Mijangos-Alquisires *et al*. (2006) reported WSSV infection in the wild *P. vannamei* and their histological work revealed typical intranuclear inclusions in the stomach epithelium. Escobedo-Bonilla *et al*. (2007) studied the pathogenesis of Thai strain of WSSV in the juvenile, specific pathogen-free *P. vannamei* and through histological studies they reported the first observation of hypertrophied nuclei and amphophilic inclusions in the foregut. Carbajal-Sanchez *et al*. (2008) studied the experimental WSSV challenge of SPF juvenile *P. vannamei* and they observed nuclear hypertrophy with karyorrhexis, pyknosis, intranuclear eosinophilic inclusions (Cowdry type A intranuclear inclusions) and intranuclear inclusion bodies with light basophilic staining. Lightner (2011) in his review on the virus diseases of farmed

shrimp showed that the WSSV intranuclear inclusion bodies are larger, without a halo in infected target tissues during the advanced stages of infection which distinguished WSSV from IHHNV. The study of Haq *et al*. (2012) revealed degenerated cells characterised by intranuclear inclusions in the tissues of WSSV infected gut epithelium. Pazir *et al*. (2012) studied the histopathology of WSSV infection in *P. vannamei* and the study showed vacuolisation of B cells and increase in the number of F and R cells, without Cowdry type A intranuclear inclusion bodies in hepatopancreas and hypertrophy and intranuclear inclusion bodies in columnar cells of mid gut. Ahmad *et al*. (2017) observed degeneration of tubular lumen, sloughing of cells with necrosis, extensive fibrosis, cell elongation, detachment of hepatopancreatic cells and necrosis of connective tissues from WSSV infected *P. vannamei*.

Pathogenesis of monodon baculovirus (MBV) has been extensively studied by Lightner *et al.* (1983) in *P. monodon* and their histological study showed nuclear hypertrophy, peripheral nucleolar displacement and chromatin rarefaction and margination in the hepatopancreatocytes. Nash *et al*. (1988) reported slight focal to severe extensive necrosis and sloughing of hepatopancreatic tubules and duct epithelium, with single to multiple spherical eosinophilic intranuclear MBV occlusions in *P. monodon*. The histological study of Fegan *et al*. (1991) in hatchery reared larvae of *P. monodon* by MBV showed the absence of occlusion bodies in the generative E-cells at the distal end of HP tubules. Vijayan *et al*. (1995) studied the prevalence and histopathology of MBV in *P. monodon* and *P. indicus* and their study showed areas of focal to extensive necrosis in the tubular epithelium along with single to multiple eosinophilic occlusion bodies in the epithelium. Ramasamy *et al*. (2000) studied the histology of MBV-infected *P. monodon* brooders and larvae and their study revealed necrosis in the tubular epithelium of hepatopancreas and multiple eosinophilic occlusion bodies in the hepatopancreatic tubules and the anterior midgut epithelial cells apart from the nuclear hypertrophy and vacuolation of hepatopancreatocytes. Gangnonngiw *et al*. (2010) reported multiple intranuclear occlusion bodies in the tissue sections of PL of *Macrobrachium rosenbergii*. Bahari *et al*. (2015) studied the histology of experimentally infected P*. vannamei* by MBV

and noticed hypertrophied nucleus with single to multiple eosinophilic occlusion bodies in the hepatocytes with mild degenerative changes.

Lightner and Redman (1985) reported hepatopancreatic parvovirus (HPV) infection in different species of shrimp and the histological study revealed densely basophilic intranuclear inclusions of HPV in the nuclei of distal hepatopancreatic tubule epithelial cells surrounded by a thin empty halo and rare occurrence of basophilic inclusion bodies in the hypertrophied nuclei of anterior midgut cells. Lightner (1996), in his book on shrimp pathology and diagnostic procedures for shrimp pathology, characterized HPV infection histologically by the presence of single, large basophilic intranuclear inclusion bodies in hypertrophied nuclei of E-cells (embryonic cells) of hepatopancreatic tubules and adjacent midgut cells. Histological analysis of HPV by Sukhumsirichart *et al*. (1999) in *P. monodon* showed the occurrence of two or more basophilic inclusion bodies in the hypertrophied E-cells nuclei. Manivannan *et al*. (2002) studied the histopathology of multiple viruses-infected postlarvae and they noticed strongly basophilic inclusion bodies indicative of HPV in the nuclei of hepatopancreatic cells along with the multiple occlusions of MBV. Catap *et al*. (2003) reported the histological analysis of the naturally infected PL by HPV and observed the basophilic intranuclear inclusion bodies in the hypertrophied nuclei of E-cells along with displacement of nucleoli. Catap and Travina (2005) studied the histology of experimentally infected *P. monodon* juveniles by HPV and the study showed both the developing intranuclear inclusions during the early stage and the large deeply basophilic, single intranuclear inclusions in the epithelial cells of distal tubules. Janakiram *et al*. (2013) performed histopathological studies on the monodon slow growth affected shrimps and their study revealed the presence of basophilic intranuclear inclusion bodies with crescent shaped nuclei pushed to one side of the nucleolus characteristic of HPV infection and the presence of polyhedral eosinophilic occlusion bodies characteristic of MBV infection in the hepatopancreatic cells.

Lightner *et al*. (1995) reported the histopathological signs of TSV in *P. vannamei* and their study revealed the multifocal areas of necrosis in the cuticular

epithelium of hindgut and stomach. The histological analysis of TSV by Hasson *et al*. (1999) showed presence of pyknotic nuclei and intranuclear inclusions along with areas of necrosis in the cuticular epithelium and subcuticular connective tissue in the posterior stomach of naturally and experimentally infected *P. vannamei* in acute phase of the TSV infection. The same authors have studied the disease cycle of TSV in *P. vannamei* and their study reported the histopathological changes occurring at the target tissues of TSV during different phases of infection. Yu *et al*. (2000) reported outbreak of TSV in *P. vannamei* and the study reported necrotic areas in the cuticular epithelium and subcutis of the foregut. Lightner (2011), in his review on the virus diseases of farmed shrimp, showed the multifocal areas of necrosis in the cuticular epithelium of foregut and hindgut during the acute phase infection of TSV.

2.2 Histopathological changes due to bacterial infections

Besides viral diseases, many bacterial diseases such as vibriosis, acute hepatopancreatic necrosis disease (AHPND), necrotizing hepatopancreatitis (NHP) are known to affect the hepatopancreas and cause histopathological changes. Vibriosis in shrimp caused by bacteria belonging to family *Vibrionaceae* is one of the major disease problems that can cause mortality in both hatchery and grow-out systems. Initially, the response of brown shrimp (*Penaeus aztecus*) to infection with *Vibrio anguillarum* and the tendency of the bacteria to concentrate in hepatopancreas were studied by Lewis (1973). Later on, Anderson *et al*. (1988) reported the poor vacuole formation in hepatopancreas due to bacterial septicemia in *P. monodon.* Jiravanichpaisal *et al*. (1994) observed septic haemocytic nodules in various organs including hepatopancreas of the shrimp with systemic vibriosis. Robertson *et al.* (1998) conducted experimental infections with *V. harveyi* in *L. vannamei* and reported the formation of bundles of necrotic tissue within the hepatopancreas followed by emaciation. Frelier *et al*. (1992) studied the histology of hepatopancreas in pacific white shrimp affected with the necrotizing hepatopancreatitis (NHP) and reported the major features such as atrophy,

multifocal necrosis and inflammation of the hepatopancreas in the infected shrimp. Later, Lightner and Redman (1994) reported massive infections of hepatopancreas by a pleomorphic intracellular Gram-negative bacterium which was named as Peru NHP (PNHP).

Recently, a new bacterial disease named acute hepatopancreatic necrosis disease (AHPND) or early mortality syndrome (EMS) has emerged causing severe mortalities in farmed *P. monodon* and *L. vannamei* in many Southeast Asian countries. Tran *et al. (*2013*)* confirmed the aetiology of AHPND as bacteria subsequent to a laboratory challenge study and the researchers identified one of the isolates of *V. parahemolyticus* infected by bacteriophage as the causative agent of AHPND. Histological observations of Lightner *et al.* (2013) in the shrimp affected by AHPND revealed the acute progressive degeneration of the HP along with the reduction of R-, B- and F cells and prominent karyomegaly and rounding and sloughing of mucosal cells into the HP tubule lumens. Soto-Rodriguez *et al*. (2015) provided field and experimental evidence of *V. parahaemolyticus* as the causative agent of AHPND in *P. vannamei*. The authors have reported major histological changes such as severe necrosis and massive sloughing of tubule epithelium with total loss of structure apart from the elongation of epithelial cells into tubular lumen and resemblance of the cells to ‘drops’ during the initial stages of infection. Leobert *et al*. (2017) studied the mortality of *P. vannamei* associated with AHPND and noticed necrotic sloughing of undifferentiated cells of hepatopancreatic tubules with the absence of basophilic bacterial cells.

2.3 Histopathological changes due to parasitic infections

Anderson *et al.* (1989) reported the microsporidian infection for the first time in hepatopancreas of shrimp which recorded the presence of spores and dilated hepatopancreatic tubules in the juvenile *P. monodon*. Chayaburakal *et al.* (2004) observed the necrosis of hepatopancreatic tubules and tubular atrophy following infection with multinucleated plasmodia of unidentified microsporidians in *P.*

monodon. Tourtip *et al*. (2009) noticed tubule epithelial cells with cytoplasmic, basophilic inclusions in the hepatopancreas of *P. monodon* infected with *Enterocytozoon hepatopenaei* (EHP). EHP-generated acute progressive degeneration of tubule mucosal cells with prominent karyomegaly and rounding and sloughing of epithelial cells into the tubule lumen was noticed in *P. vannamei* by Lightner (2012). Tangprasittipap *et al*. (2013) revealed the spore formation in the B cells of hepatopancreatic tubule epithelium of *P. vannamei* while studying the causative agent of white feaces syndrome (WFS) in farmed *P. vannamei*. Sriurairatana *et al.* (2014) studied the WFS in *P. vannamei* and *P. monodon* and reported the transformation, sloughing and aggregation of hepatopancreatic microvilli into vermiform bodies resulting in atrophied transformed microvilli (ATM). Tang *et al.* (2015) showed inclusions of plasmodium and mature spores of EHP in naturally infected *P. vannamei.* Salachan *et al*. (2016) studied the laboratory co-habilitation model for EHP in *P. vannamei* and showed the presence of spores and plasmodia in the epithelial cells of central region of the hepatopancreas. Recently, Rajendran *et al.* (2016) described the histopathological changes caused by EHP in hepatopancreas of *P. vannamei* farmed in India for the first time. Tang *et al.* (2016) showed the presence of spores of EHP in hepatopancreas and midgut epithelium of *P. vannamei* affected with WFS, which formed the first report on the presence of EHP spores in the midgut epithelial tissues. Biju *et al*. (2016) reported high prevalence of EHP in shrimp exhibiting slow growth and their report showed the early and late plasmodial stages and mature spores in the tubule epithelial cells of the hepatopancreas. Santhoshkumar *et al*. (2016) revealed the presence of basophilic plasmodium within the vacuoles in HP tubule cytoplasm and in the tubule lumen of *P. vannamei* subsequent to infection with EHP. Aranguren *et al.* (2017) recorded prominent histological changes caused by *E. hepatopenaei* in the medial and proximal regions of the hepatopancreas in *P. vannamei*. Kummari *et al.* (2018) studied the incidence of EHP in the *P. vannamei* farms and observed the sloughing of epithelial cells and detachment of tubules of the hepatopancreas. Janakiram *et al*. (2018) conducted aetiological studies on mixed infection of abdominal segment

deformity disease (ASDD) and EHP in farmed *P. vannamei* and the histopathological study reported hypertrophy and degeneration of hepatopancreatic tubules.

2.4 Histopathological effects caused by abiotic factors

Apart from various pathogens, some of the abiotic factors causing alterations in normal well-being of farmed shrimp have been studied. Sreeram *et al*. (2005) evaluated the adverse effect in the hepatopancreas due to exposure to petroleum hydrocarbons in *Metapenaeus dobsonii.* They reported vacuolation of E-cell layers and proliferation of R-cells, breakage of tubule connective tissue lining and sloughing off of the tubule epithelium. Stentiford and Feist (2005) conducted a histological survey in which histopathological changes in the hepatopancreas were described in shore crab (*Carcinus maenas*) and brown shrimp (*Crangon crangon*) from six estuaries in the United Kingdom. Sousa *et al*. (2007) used histopathological techniques to study the influence of environmental pollution with pesticides in the functional morphology of the hepatopancreas in the decapod *Palaemonetes argentinus.* Diaz *et al.* (2010) studied the functional cytology of the hepatopancreas of *P. argentinus* under osmotic stress and revealed the enlarged tubular lumen and an infolded basal lamina in the shrimp.

MATERIALS AND METHODS

3. MATERIALS AND METHODS

3.1 Collection of samples:

3.1.1 Sample collection site:

The shrimp samples were sourced from shrimp farms located in Palghar and Raigad districts of Maharashtra (brackishwater farms) and in Rohtak district of Haryana (inland saline farms) culturing *Penaeus (L.) vannamei*. Three farms each were selected for the study from each state. A total of 6 farms were selected for sample collection representing 3 brackishwater and 3 farms inland saline farms. The geographical location of the farms selected for sample collection in Maharashtra and Haryana are given in Fig.1 & Fig.2 respectively

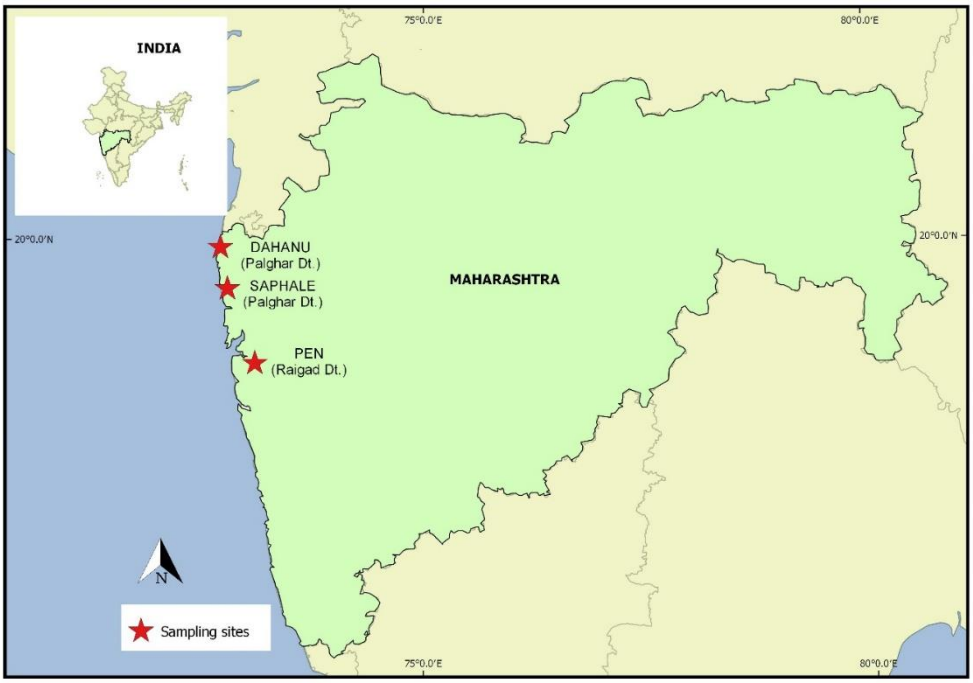

Fig.1. Sample collection sites in Maharashtra - Dahanu (19°57'52.0"N 72°42'54.5"E), Saphale (19°31'31.4"N 72°47'56.4"E) and Pen (18°43'58.5"N 73°06'56.7"E)

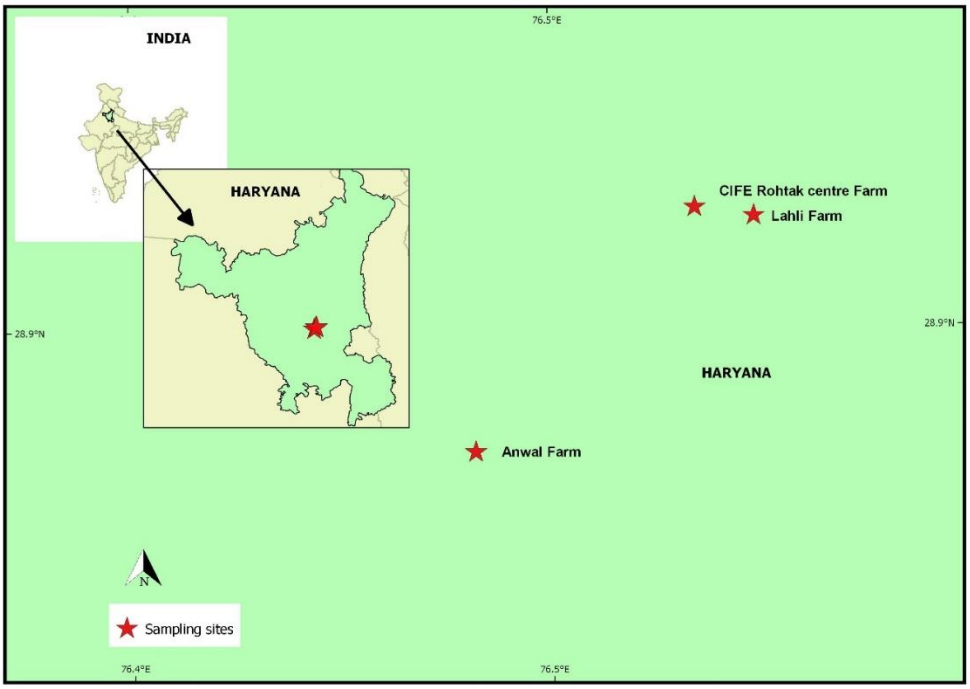

Fig. 2. Sample collection sites in Haryana (Rohtak district) - CIFE Rohtak centre (28°51'41.8"N 76°28'27.7"E), Lahli (28°51'45.2"N 76°28'02.3"E), and Anwal (28°50’13.2” N 76°26’27.3” E)

3.1.2 Sample collection from Maharashtra:

A total of 30 animals (size: 8.4-27.6 g) were randomly collected from three farms. The sampling was done during the period August 2017 to January 2018 and preserved in Davidson’s fixative, following the procedure of Bell and Lightner (1988), by injecting 1 to 2 mL of the fixative into the cephalothorax region of live shrimp (whole head soft tissue) using 1 mL insulin syringe. Further, the carapace was removed and the cephalothorax region of shrimp along with the dissected intestine was transferred to 50 mL Falcon tubes containing fixative. Simultaneously, 10 shrimp from each farm were collected for molecular diagnosis. These animals were stored immediately in the Styrofoam boxes containing dry ice. All the collected samples were transported to the Laboratory of Aquatic Environment and Health Management Division, Central Institute of Fisheries Education (CIFE), Mumbai. The samples preserved in Davidson’s fixative at room temperature were transferred to

70% alcohol after 48 h. The frozen shrimps in dry ice were kept at -80 °C until further use.

3.1.3 Sample collection from Rohtak:

P. vannamei were collected from 3 farms (ICAR-CIFE, Rohtak Centre farm, Lahli and Anwal farms). Two ponds from each farm were randomly selected and five animals from each pond (size: 9.0 to 18.0 g) were collected and subsequently transported in live condition to the Aquatic Animal Health laboratory of CIFE Centre, Rohtak.

A total of 30 animals were collected and hepatopancreas and gut were aseptically dissected out and small portion of the hepatopancreas and gill tissue was collected in 100% ethanol (Sigma – Aldrich) for the extraction of DNA. The rest of the tissues were immediately fixed in Davidson's fixative for 48 h at room temperature. The fixed tissues were transferred to 70% ethanol and the samples were allowed to remain in ethanol until processing for histology. The collected samples were transported to Aquatic Animal Health Laboratory, CIFE, Mumbai, for further analysis.

3.2 Histology:

The whole head soft tissues of shrimp collected from farms in Maharashtra as well as hepatopancreas and gut tissues collected from farms in Haryana were processed according to the procedure described in Bell & Lightner (1988). The tissue processing includes dehydration, clearing and preparation of paraffin embedded tissue blocks. Tissues were dehydrated in ethanol series from 70%, 80%, 90% and 100% with a dehydration time of 1.5 h each. The clearing step was carried out by immersion of tissues in xylene for 1.5 h. A second immersion in xylene for 1.5 h was given before transferring the tissues into molten paraffin at 65°C (embedding medium) for 3 h. Additional paraffin infiltration step was performed for 3 h prior to embedding of tissues using tissue embedding system (Leica EG 1140C, Germany)

Tissue sections (3 - 6 µm) were taken using a rotary microtome (Leica RM2125RT, Germany) and subsequently, allowed to stretch in water bath maintained at 40 - 45°C. The tissue ribbon was then taken on egg albumen coated glass slides followed by drying at room temperature (overnight) before staining them with Mayer's hematoxylin and Eosin-Phloxin solution.

Tissue sections spread on the slides were immersed in xylene for 12 to 15 h for de-paraffinization and staining was performed following the standard protocol (Bell and Lightner 1988). In brief, the slides were immersed in Coplin jar containing xylene for 30 min and gradual hydration of tissue sections was performed by keeping the slides in graded ethanol series of 100%, 90%, 70%, 50% and tap water for 15 min each. Subsequently, the slides were immersed in Mayer's hematoxylin for 40 sec. followed by a wash in tap water for 10 min. A dip in acid alcohol, tap water and Scott's tap water was performed to remove excess hematoxylin. After adequate staining with hematoxylin, the slides were dehydrated in graded ethanol series of 50%, 70%, 90% and 100% ethanol for 15 min in each solution before an eosin dip. Then, the slides were further dehydrated by incubation in 100% ethanol for 1 h, acetone plus 100% ethanol for 30 min and acetone for 30 min. Finally, the slides were immersed in xylene for 1 h prior to mounting in DPX (Hi-Media, India). Stained slides were observed under upright light microscope (Carl Zeiss, Germany) and photographs were captured at 4X, 10X and 100x magnifications using TCapture software.

3.3 Genomic DNA isolation:

The hepatopancreas and few gill tissue collected from shrimp were subjected to DNA extraction following modified CTAB extraction method (standardized in the labaratory). The tissue samples were taken in a sterile 1.5 mL micro centrifuge tube containing 570 µL of lysis buffer (Appendix). The tissues in lysis buffer were incubated overnight at -80 °C and were homogenized using sterile micro pestle. Later, the homogenate was incubated at 37°C for 30 min following the addition of 10 µL lysozyme and 5 µL of RNase A (Appendix). Next, 30 µL of 10%

SDS stock and 10 µL of Proteinase K (Appendix) were added followed by incubation at 55 °C for 1 h with continuous shaking in rotary shaking water bath (Expo Hi-Tech, India). Thereafter, 120 µL of pre-warmed 5 M NaCl and 96 µL of 10% CTAB were added to the tubes followed by incubation at 65°C for 10 min in water bath. Subsequently, 700 µL of chloroform:isoamyl alcohol (24:1) was added to the tubes and the samples were centrifuged at 16,000 xg for 5 min at room temperature. The resulting supernatant was collected in fresh 1.5 mL tubes without disturbing the interphase. Next, ice cold Isopropanol (0.7 volumes of aqueous phase) was added to the transferred supernatant solution to precipitate the DNA. The mixture was allowed to stand for 2 h at RT to facilitate complete precipitation of DNA. Later, the tubes were centrifuged at 21,000 xg for 30 min at RT to pellet the precipitated DNA. The resulting pellet was washed by adding 400 µL of 70% ethanol. The ethanol was removed by centrifugation at 21,000 xg for 5 min and the DNA pellets was suspended in 30 µL of nuclease free water. The isolated DNA was stored at -20°C for long term storage after quantification using Nanodrop® spectrophotometer (Thermo Scientific, USA).

3.4 PCR amplification:

On the basis of histopathological changes in hepatopancreas and gut, possible causative agents were shortlisted using the data from the previous studies (Lightner *et al*., 1983; Lightner and Redman., 1985; Lightner, 1995; Lightner, 1996; Lightner *et al*., 2013). Accordingly, the pathogens such as EHP, WSSV, IHHNV, HPV, MBV, VP_{AHPND} and NHP-bacterium were selected for PCR-based screening.

3.4.1 Composition of PCR master mix:

DNA extracted from different tissues were subjected to PCR. A 25 µL PCR reaction mixture was used which consisted of 2.5 µL (10X PCR reaction buffer), 1 µL $MgCl_2$ (50 mM), 0.5 µL dNTP mix (10 mM), 0.5 µL (25 pM/ µL) forward and reverse primers of respective PCR, 0.25 µL Taq DNA polymerase (5 U) (Invitrogen®), 2.0 µL template DNA (equivalent to 50 ng) and 17.75 µL of nuclease-

free water. In case of Nested PCR, 2 µL of first step PCR product was taken as template for the second step and the PCR was carried out as mentioned in the earlier section

3.4.2 Primers used for detection:

PCR amplification was performed to detect EHP, WSSV, IHHNV, HPV, MBV, VP$_{AHPND}$ and NHP-bacterium from selected samples. The oligo-nucleotides primers were selected on the basis of various published works and their specificity to detect the target pathogens. The details of the primer sequences are given in Table.1 and the cycling conditions for PCR amplification of the different target genes are given in Table.2 to Table.11.

Table 1. List of primers used for detection of various pathogens

Target Gene	Primer Name	Primer sequence (5'-3')	Amplicon size (bp)	Reference
Spore Wall Protein	SWP 1F	TTGCAGAGTGTTGTTAAGGGTTT	514	Jaroenlak *et al.* (2016)
	SWP 1R	CACGATGTGTCTTTGCAATTTTC		
	SWP 2F	TTGGCGGCACAATTCTCAAACA	148	Jaroenlak *et al.* (2016)
	SWP 2R	GCTGTTTGTCTCCAACTGTATTTGA		
WSSV *Sal* I	146 F2	GTAACTGCCCCTTCCATCTCCA	941	Nunan & Lightner (2011)
	146 R2	TACGGCAGCTGCTGCACCTTGT		
IHHNV NSP 1	IHHNV 309 F	TCCAACACTTAGTCAAAACCAA	309	OIE
	IHHNV 309 R	TGTCTGCTACGATGATTATCCA		
NHP 16S rRNA	NHP F2	CGTTGGAGGTTCGTCCTTCAGT	379	Nunan & Lightner (2008)
	NHP R2	GCCATGAGGACCTGACATCATC		

MBV	MBV F1	CGATTCCATATCGGCCGAATA	533	OIE
	MBV R1	TTGGCATGCACTCCCTGAGAT		
	MBV F2	TCCAATCGCGTCTGCGATACT	361	OIE
	MBV R2	CGCTAATGGGGCACAAGTCTC		
HPV	HPV 400F	TTCCAGGAAGAAGGACAAAATCATT	400	In the Laboratory of AAHM
	HPV 400R	CGTGGCGCTGGAATGAATC		
pVA plasmid of VP_{AHPND}	AP4-F1	ATGAGTAACAATATAAAACATGAAAC	1269	Dangtip *et al.* (2015)
	AP4-R1	ACGATTTCGACGTTCCCCAA		
	AP4-F2	TTGAGAATACGGGACGTGGG	230	
	AP4-R2	GTTAGTCATGTGAGCACCTTC		

Table.2. Thermal Regime for SWP 1F & 1R primers (1st Step)

Steps	Conditions		Cycles
	Temperature	Time	
Initial Denaturation	95ºC	5min.	1 Cycle
Denaturation	95ºC	30sec.	30 Cycles
Annealing	58ºC	30sec.	
Extension	68ºC	45sec.	
Final Extension	68ºC	5min.	1 Cycle
Hold	4ºC	∞	-

Table.3. Thermal Regime for SWP 2F & 2R Primers (2nd Step)

Steps	Conditions		Cycles
	Temperature	Time	
Initial Denaturation	95ºC	5min.	1 Cycle
Denaturation	95ºC	30sec.	20 Cycles
Annealing	64ºC	30sec.	
Extension	68ºC	45sec.	
Final Extension	68ºC	5min.	1 Cycle
Hold	4ºC	∞	-

Table 4. Thermal Regime for WSSV 146 F2 & R2 Primers

Steps	Conditions		Cycles
	Temperature	Time	
Initial Denaturation	94ºC	5min.	1 Cycle
Denaturation	94ºC	30sec.	40 Cycles
Annealing	62ºC	30sec.	
Extension	72ºC	45sec.	
Final Extension	72ºC	5min.	1 Cycle
Hold	4ºC	∞	-

Table 5. Thermal Regime for IHHNV 309 F & R Primers

Steps	Conditions		Cycles
	Temperature	Time	
Initial Denaturation	94ºC	5min.	1 Cycle
Denaturation	94ºC	30sec.	40 Cycles
Annealing	55ºC	30sec.	
Extension	72ºC	45sec.	
Final Extension	72ºC	5min.	1 Cycle
Hold	4ºC	∞	-

Table 6. Thermal Regime for NHP F2 & R2 Primers

Steps	Conditions		Cycles
	Temperature	Time	
Initial Denaturation	95ºC	5min.	1 Cycle
Denaturation	95ºC	30sec.	40 Cycles
Annealing	60ºC	30sec.	
Extension	72ºC	45sec.	
Final Extension	60ºC	1min.	1 Cycle
	72ºC	2min.	
Hold	4ºC	∞	-

Table 7. Thermal Regime for MBV F1 & R1 Primers (1st step)

Steps	Conditions		Cycles
	Temperature	Time	
Initial Denaturation	96ºC	5min.	1 Cycle
Denaturation	94ºC	30sec.	40 Cycles
Annealing	65ºC	30sec.	
Extension	72ºC	30sec.	
Final Extension	72ºC	7min.	1 Cycle
Hold	4ºC	∞	-

Table 8. Thermal Regime for MBV F2 & R2 Primers (2nd step)

Steps	Conditions		Cycles
	Temperature	Time	
Initial Denaturation	96ºC	5min.	1 Cycle
Denaturation	94ºC	30sec.	35 Cycles
Annealing	60ºC	30sec.	
Extension	72ºC	60sec.	
Final Extension	72ºC	7min.	1 Cycle
Hold	4ºC	∞	-

Table 9. Thermal Regime for HPV 400 F & R Primers

Steps	Conditions		Cycles
	Temperature	Time	
Initial Denaturation	95ºC	5min.	1 Cycle
Denaturation	95ºC	1min.	35 Cycles
Annealing	60ºC	1min.	
Extension	72ºC	1min.	
Final Extension	72ºC	7min.	1 Cycle
Hold	4ºC	∞	-

Table 10. Thermal Regime for AP4 F1 & R1 Primers (1st step)

Steps	Conditions		Cycles
	Temperature	Time	
Initial Denaturation	94ºC	2min.	1 Cycle
Denaturation	94ºC	30sec.	35 Cycles
Annealing	55ºC	30sec.	
Extension	72ºC	90sec.	
Final Extension	72ºC	2min.	1 Cycle
Hold	4ºC	∞	-

Table 11. Thermal Regime for AP4 F2 & R2 Primers (2nd step)

Steps	Conditions		Cycles
	Temperature	Time	
Initial Denaturation	94ºC	2min.	1 Cycle
Denaturation	94ºC	20sec.	25 Cycles
Annealing	55ºC	20sec.	
Extension	72ºC	20sec.	
Final Extension	72ºC	2min.	1 Cycle
Hold	4ºC	∞	-

3.5 Agarose gel electrophoresis:

The PCR-amplified products were electrophoresed on agarose gel. For this, 1.5% agarose gel was prepared in 0.5 X TAE (Tris – Acetate – EDTA) buffer containing ethidium bromide (0.5 µg/mL). An aliquot (8 µL) of the PCR product was mixed with 2 µL of gel loading dye (6X) before loading the product onto the gel. Along with the products, a molecular size standard (Fermentas, USA) was also loaded in the gel. The electrophoresis run was performed at 120 V. for 30 min. Later, the gel was visualised and documented in a gel documentation unit (Vilber Lourmat®, Germany).

RESULTS

4. RESULTS

4.1 Histological analysis

A total of 60 specimens of farmed *Penaeus vannamei* of different sizes (8.4 - 27.6 g) collected from Haryana (inland saline water) and Maharashtra (brackishwater) were histologically analyzed. No gross pathological changes were observed in the animals collected from Haryana. However, some of the shrimp samples collected from Maharashtra showed retarded growth.

4.1.1 Hepatopancreas

Histological analysis of hepatopancreas from farmed *P. vannamei* revealed many histopathological abnormalities. The histological preparations of normal, healthy hepatopancreas were taken as standard reference. The normal hepatopancreas was characterized by intact tubular epithelium with distinct cell types in the proximal part of hepatopancreas including large basophilic F-Cells and R & B-cells with prominent vacuoles. Intertubular connectives showing myoepithelium and haemal sinuses with few haemocytes were also observed in the normal hepatopancreas. Healthy E-cells were observed at the distal part of the organ. The lumen in the proximal part appeared star-shaped (Plate 1 & 2).

Histopathological changes observed in the hepatopancreas during the present study included moderate to heavy tubular necrosis, detachment and complete sloughing of tubular epithelium, tubular atrophy, heavy haemocytic infiltration, abnormally enlarged haemal sinuses, encapsulation, nodule formation and melanisation. Histological sections also revealed developmental stages and spores of microsporidian parasite, *Enterocytozoon hepatopenaei* and bacterial colonies.

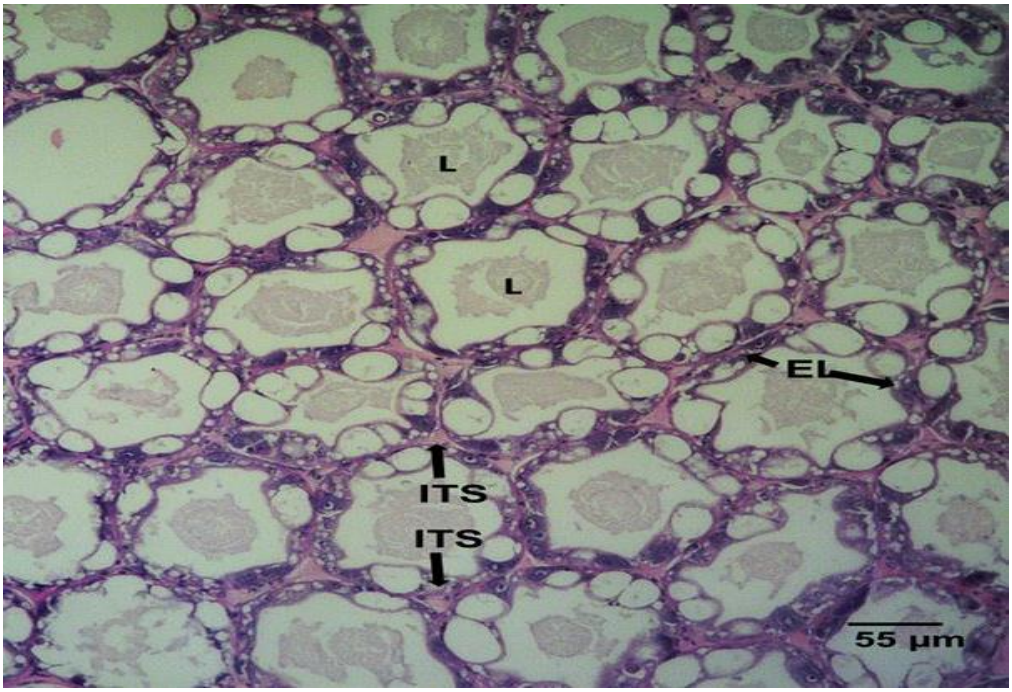

Plate 1. Histological section of hepatopancreas showing normal architecture marked by the intact epithelial layer (EL), inter-tubular connectives, haemal sinuses (ITS) and star-shaped lumen (L) containing cellophane-like material. (x 100; H&E stained)

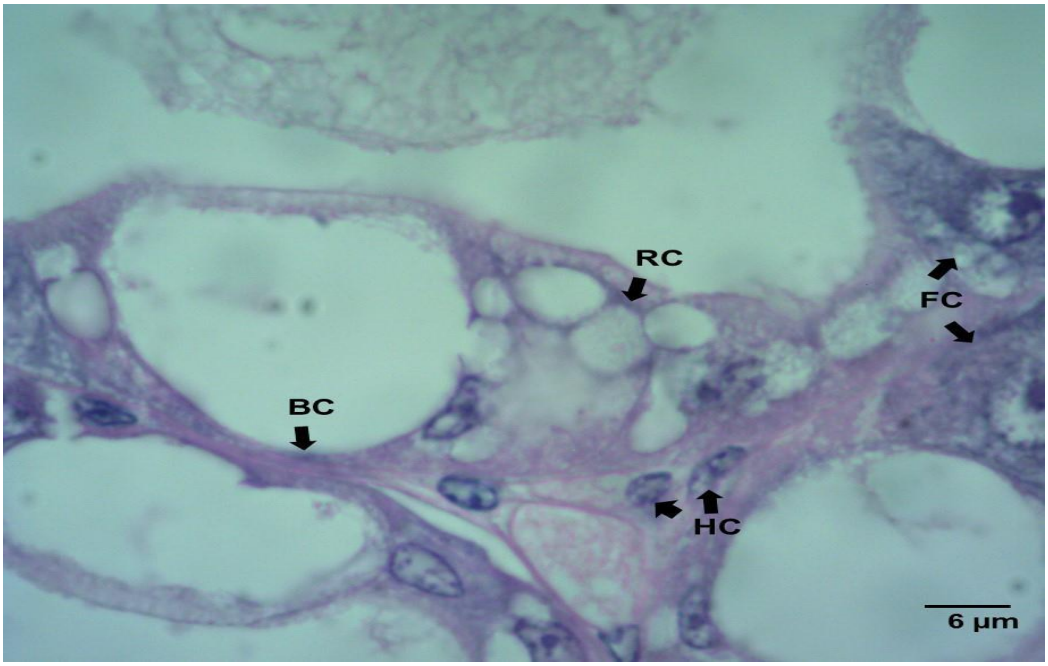

Plate 2. Histological section (Enlarged view) of hepatopancreas showing normal architecture with the intact epithelial layer with distinct cell types, inter-tubular connectives and sinuses and lumen. Arrows mark the F Cell (FC), R cell (RC), B Cell (BC) and haemocytes in the haemal sinus (HC). (x 1000; H&E stained)

4.1.1.1 Microsporidian infection

High prevalence of microsporidian infection was detected in the histological analysis of hepatopancreas and was marked by *Enterocytozoon hepatopenaei* (EHP) related pathology. Presumptive developmental stages of EHP plasmodia, were observed as deeply basophilic inclusion-like bodies in majority of HP sections. These were either observed on the vacuole or in the cytoplasm. (Plate 3 & 4). Although cellular changes such as nuclear hypertrophy and necrosis of epithelial cells of the HP tubules were noticed in tubules with microsporidian plasmodia, no haemocytic infiltration could be observed (Plate 4). However, presence of basophilic granulation in the tubular epithelial cells was noted in some cases (Plate 4A). However, in the case of heavy infection, detachment of the tubular epethlia and presence of sloughed basophilic bodies were observed in the hepatopancreatic lumen (Plate 4B).

In the advanced stages of infection, severe necrosis of hepatopancreatic tubules was noticed. Tubular epithelium containing various stages of the parasite development and hypertrophied nuclei was found to be getting detached from the underlying connectives. In some case, different stages of the necrosis process starting from partial detachment of tubules from the connective tissue and ultimately ending in the complete sloughing of the tubular epithelium and haemocytic infiltration were detected (Plate 5). In the advanced stage, no remnants of tubular epithelium was visible and the lumen contained aggregation of EHP spores surrounded by flattened haemocytic cells (Plate 5).

Histological sections of hepatopancreas of some of the animals showed structures similar to aggregated transformed microvilli (ATM) like bodies in the hepatopancreatic tubule lumen. (Plate 6). The histological sections showing the presence of ATM-like bodies did not reveal any severe haemocytic infiltration or encapsulation. Although ATM-like structures have been linked with white feces

syndrome in the past studies, no such white fecal strands were observed in the pond at the time of collection of samples.

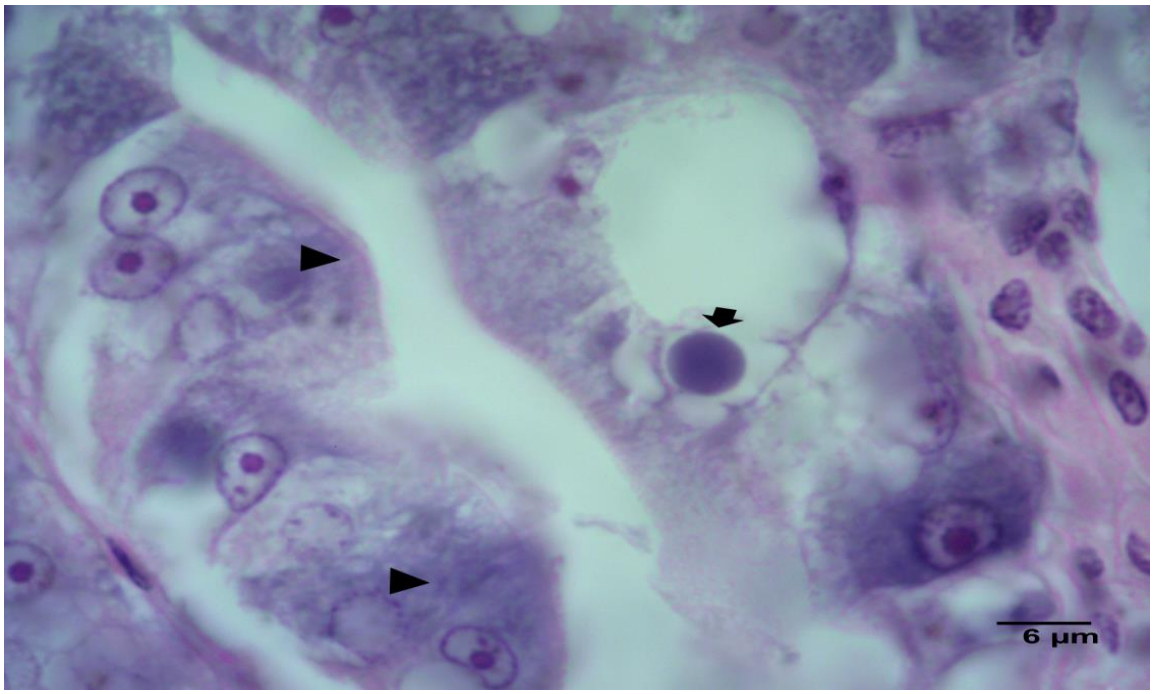

Plate 3. Histological section (Enlarged view) of hepatopancreas showing hypertrophied nuclei (arrowhead) and deeply basophilic inclusion-like body (arrow) of presumptive developmental stage of EHP (x 1000; H&E stained)

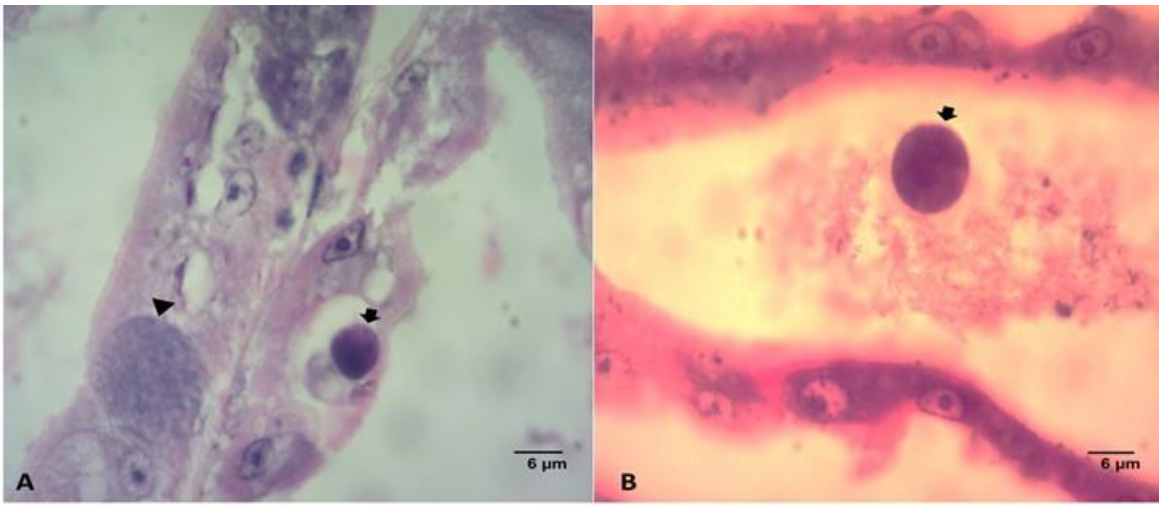

Plate 4. (A) Histological section (Enlarged view) of hepatopancreas showing deeply basophilic inclusion-like body (arrow) of presumptive developmental stage of EHP and the F cell becoming granular in nature (arrowhead). Epithelial cells show necrotic changes (x 1000; H&E stained). **(B)** Histological section (Enlarged view) of hepatopancreas showing and deeply basophilic inclusion-like body in the lumen (arrow) (x 1000; H&E stained)

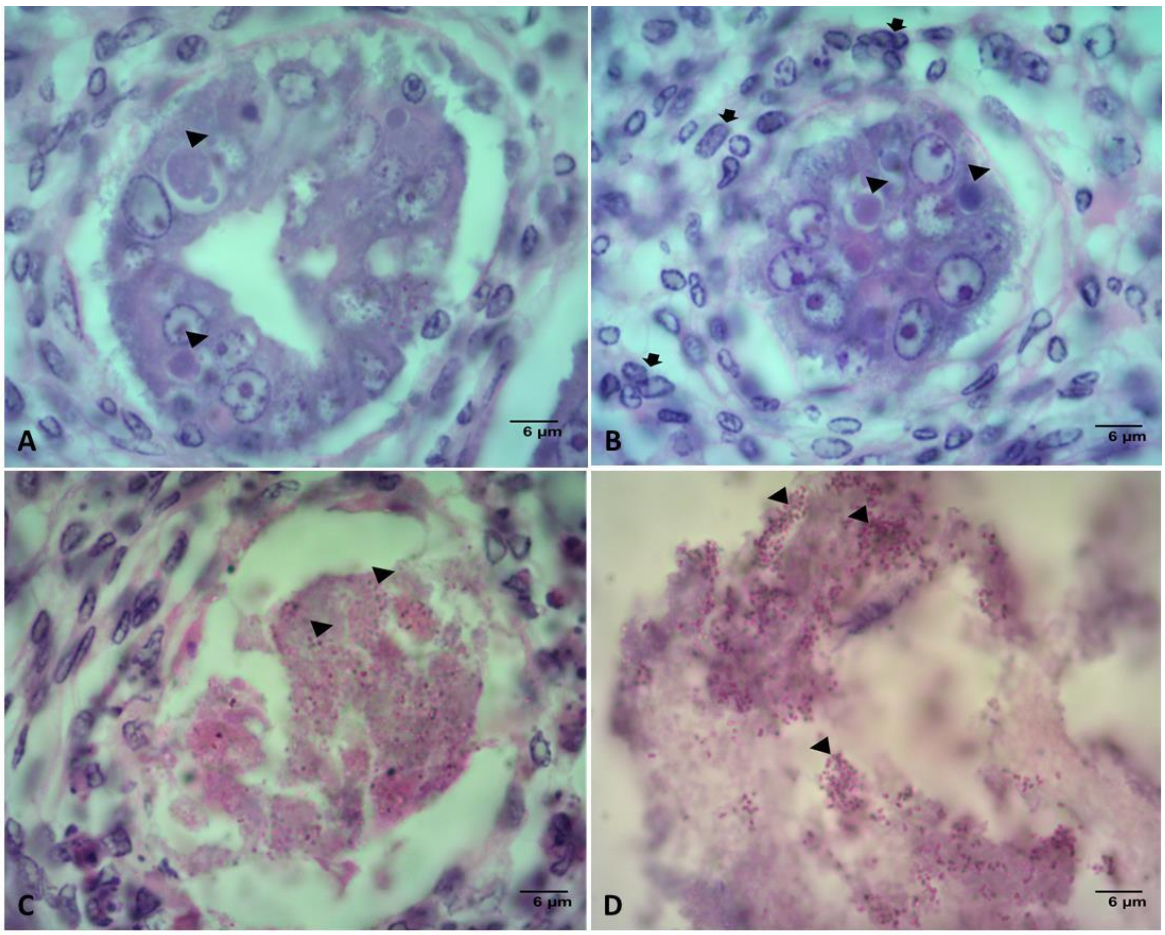

Plate 5. Different stages of tubular necrosis in hepatopancreas due EHP infection. **(A)** Histological section of hepatopancreas showing early stage of tubular necrosis and developmental stages of EHP (arrowhead) Note the partial detachment of tubular epithelium (x 1000; H&E stained). **(B)** Histological section of hepatopancreas showing advanced stage of tubular necrosis and developmental stages of EHP (arrowhead) Note the complete detachment of tubular epithelium and haemocytic infiltration in the connectives (arrows) (x 1000; H&E stained). **(C)** Histological section of hepatopancreas showing complete dissolution of epithelial cells and spores of EHP in the necrotized lumen of hepatopancreatic tubule connectives (arrowhead) (x 1000; H&E stained). **(D)** Histological section of hepatopancreas showing aggregation of spores of EHP in the necrotized lumen of hepatopancreatic tubule (arrowhead) (x 1000; H&E stained)

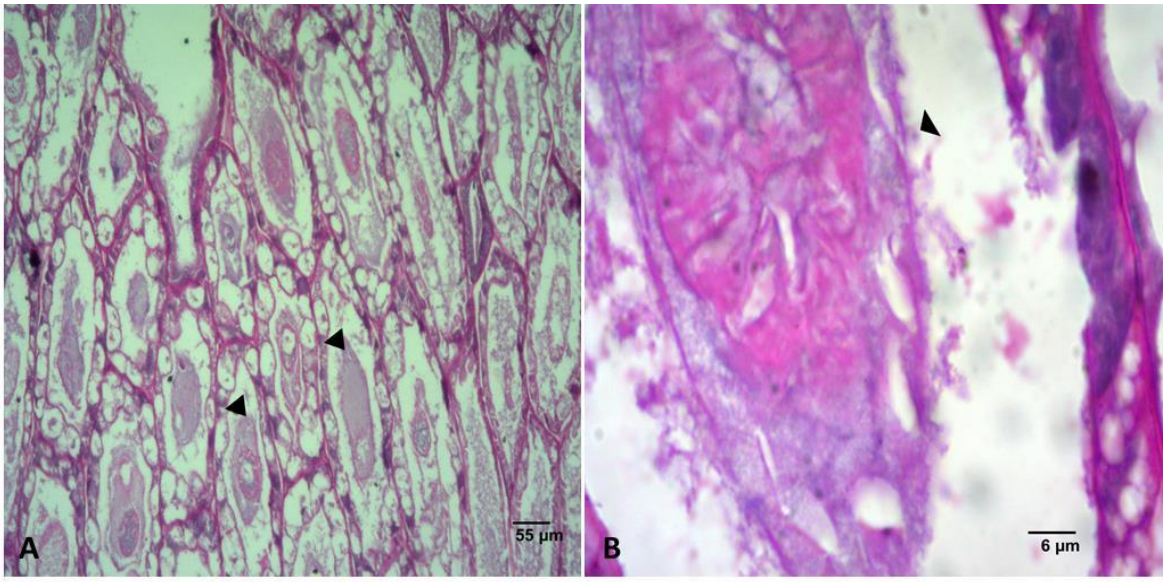

Plate 6. Aggregated Transformed Microvilli (ATM)-like bodies. **(A)** Histological section showing aggregated transformed microvilli (ATM)-like bodies in the hepatopancreatic lumen (arrowhead) (x 1000; H&E stained). **(B)** Histological section of hepatopancreas showing enlarged view of aggregated transformed microvilli (ATM)-like body in the hepatopancreatic lumen (arrowhead). Note the degenerated epithelial layer (x 1000; H&E stained)

4.1.1.2 Bacterial infection

Histopathological lesions characteristic of bacterial infection were observed in many shrimp specimens examined. Moderate to severe necrosis predominantly in the proximal and medial part of hepatopancreas was observed. In severe cases, completely atrophied tubules surrounded by abnormally enlarged haemal sinuses with heavy infiltration of haemocytes were prominent. In this case, the pathological lesions observed in the hepatopancreas resembled the pathology of AHPND. Several foci of melanised nodules characteristic of bacterial septicaemic conditions were observed (Plate 7). Further, similar severe necrosis characterized by total degeneration of hepatopancreatic tubule leading to atrophy encapsulation, nodulation and melanisation were also observed in the distal region of the hepatopancreatic region (Plate 8).

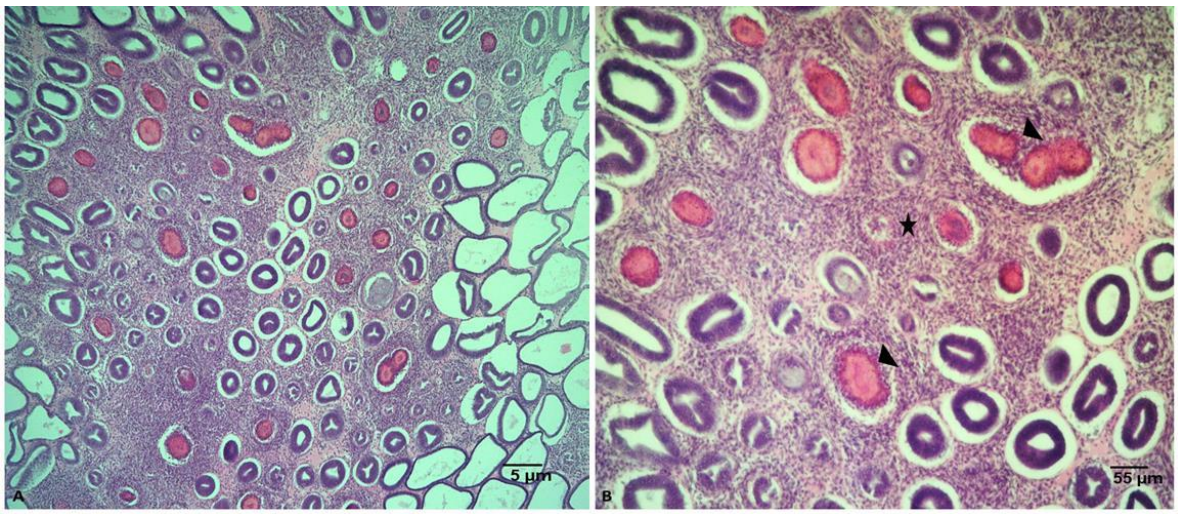

Plate 7. Hepatopancreas showing AHPND-like pathology. **(A)** Histological section of hepatopancreas showing acute hepatopancreatic necrosis (medial region). Note the abnormally enlarged haemal sinuses with haemocytic aggregation around detached, atrophied tubules. Several melanised nodules can also be seen (x 40; H&E stained). **(B)** Histological section of hepatopancreas (enlarged view) showing acute hepatopancreatic necrosis (medial region). Note the abnormally enlarged haemal sinuses with haemocytic aggregation (star shape) around detached, atrophied tubules. Several melanised nodules can also be seen (arrowhead) (x 100; H&E stained)

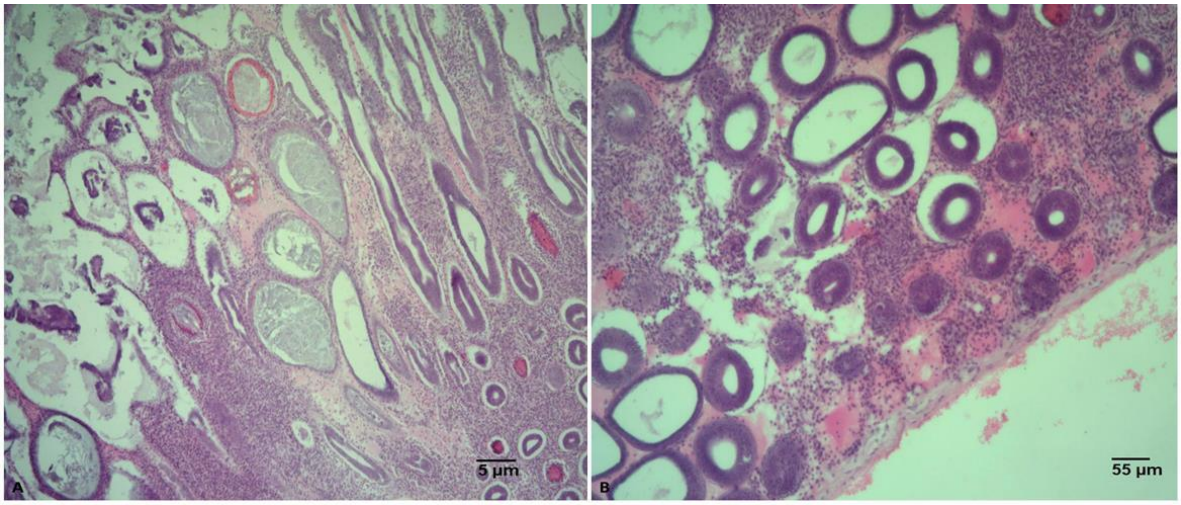

Plate 8. Acute hepatopancreatic necrosis. **(A)** Histological section of hepatopancreas showing acute hepatopancreatic necrosis (distal region). (x 40; H&E stained). **(B)** Enlarged view showing acute hepatopancreatic necrosis (distal region). Note the highly enlarged haemal sinuses with heavy haemocytic infiltration as well as completely detached tubules (x 100; H&E stained)

Another histopathological change observed in the hepatopancreas of some of the shrimp examined included enlargement of lumen due and complete degeneration of epithelial layer and the histoarchitecture appeared like a stretched net. Although detachment and atrophy of the hepatopancreatic tubules were observed, heavy infiltration of haemocytes and abnormal enlargement of haemal sinuses were not observed in these cases (Plate 9). The histopathological changes observed in these cases resembled the pathology associated with necrotizing hepatopancreatitis (NHP).

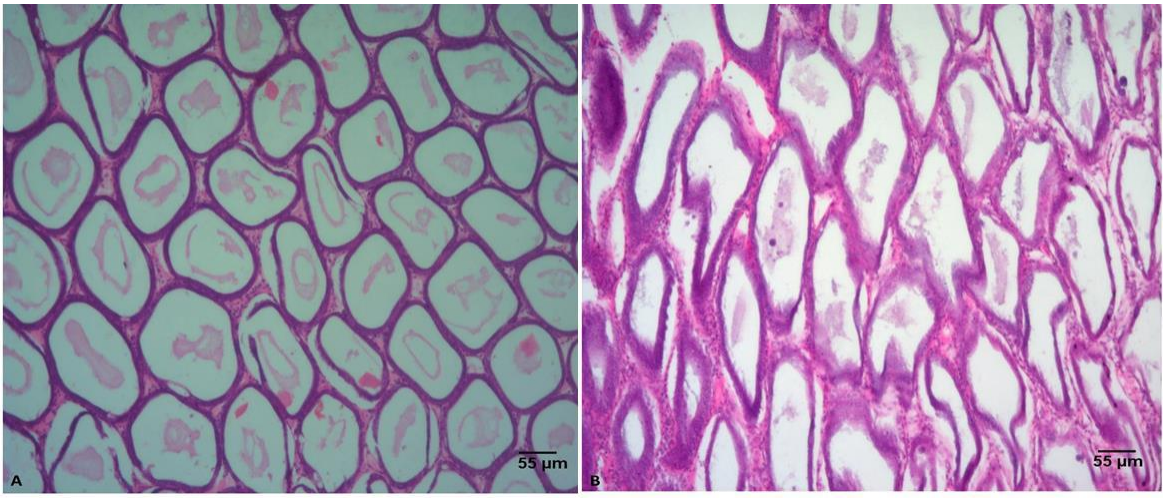

Plate 9. NHP related pathology. **(A)** Histological section of hepatopancreas showing necrotised hepatopancreatic tubule. Note the enlarged tubule lumen and the absence of enlargement of haemal sinuses & heavy haemocytic infiltration (x 100; H&E stained). **(B)** Histological section of hepatopancreas showing necrotised hepatopancreatic tubule (enlarged view). (x 100; H&E stained).

4.1.1.3 Co-infection with EHP and Bacteria

Histological sections of hepatopancreas showing co-infection with EHP and bacteria were also observed during the present survey. The sections of HP with dual infection showed various stages of necrosis accompanied by encapsulation with haemocytes and nodule formation and melanisation. Different stages of the necrotic changes leading to the formation of melanised nodules are depicted in Plate 10.

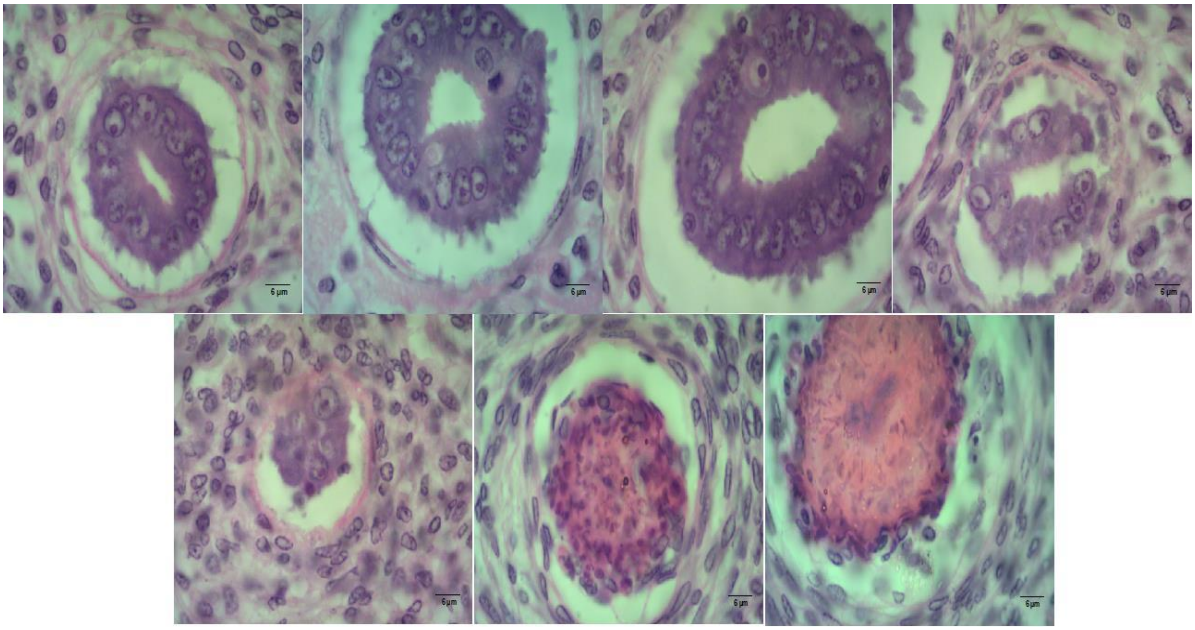

Plate 10. Histological sections of hepatopancreas showing different stages of encapsulation, nodule formation and melanisation (x 1000; H&E stained)

One of the interesting observations made in the present study was the identification of colonies of rod-shaped bacteria in the lumen of hepatopancreas (Plate 11) and co-occurrence of EHP sores along with the bacterial colonies in the sloughed material in the lumen (Plate 12).

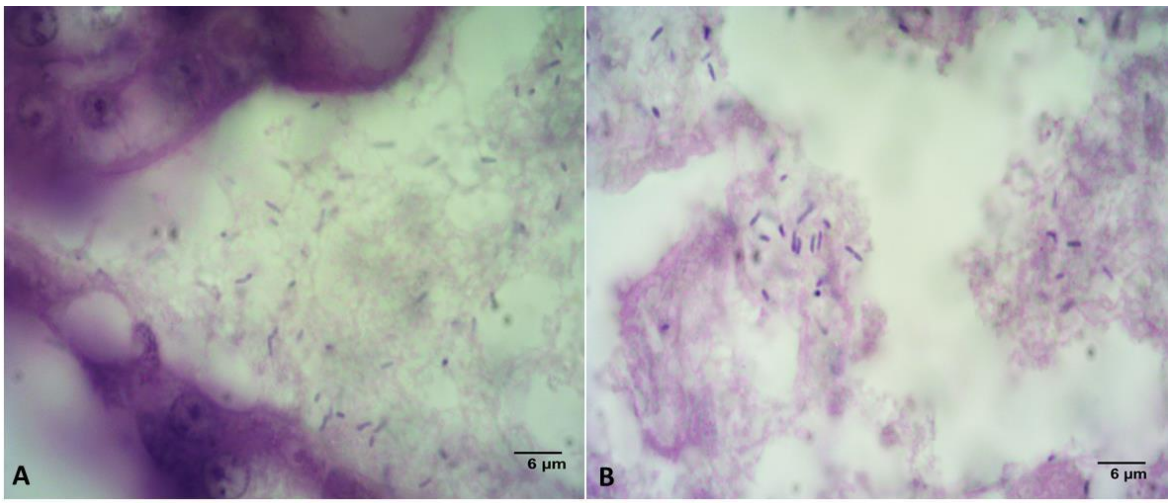

Plate 11. Rod-shaped bacteria in hepatopancreas. **(A)** Histological section of hepatopancreas showing the rod-shaped bacteria in the hepatopancreatic lumen (x 1000; H&E stained). **(B)** Another section of hepatopancreas showing distinct rod-shaped bacteria in the sloughed material in the hepatopancreatic lumen (x 1000; H&E stained).

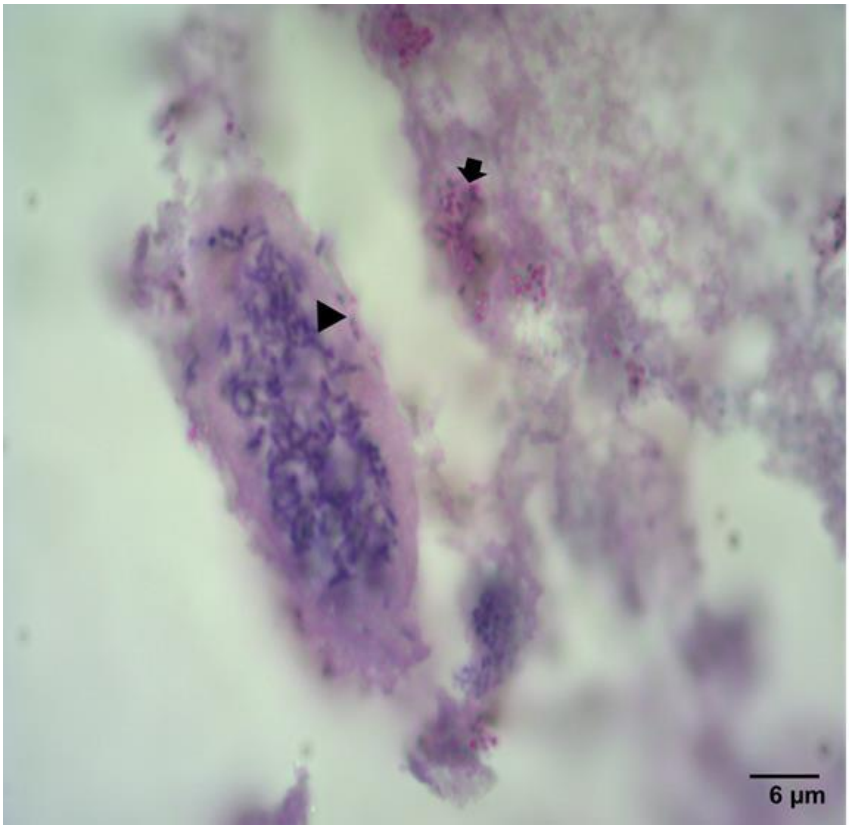

Plate 12. Histological section of hepatopancreas showing the rod-shaped bacteria (arrowhead) and EHP spores (arrow) in the hepatopancreatic lumen(x 1000; H&E stained)

4.1.1.4 Viruses

No virus-associated pathology could be detected in any of the histological sections of either hepatopancreas or gut. Hepatopancreas also showed no inclusion bodies characteristics of MBV and HPV.

4.1.2 Gut

Majority of the gut samples examined did not reveal any major pathological alterations. The normal histological features of different parts of gut observed are given in Plate 13 & 14.

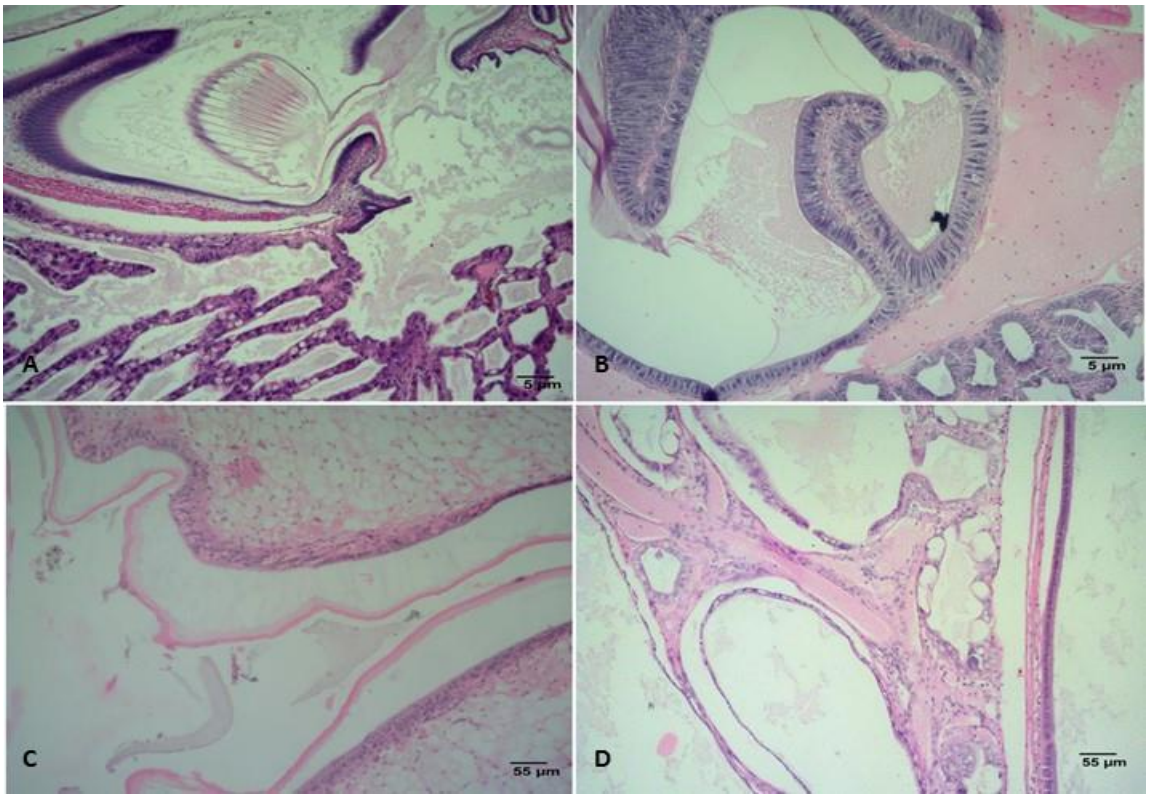

Plate 13. Normal gut histology. Histological section showing the gut (stomach, midgut and hindgut regions) with normal intact epithelium.(A&B- X 40; H&E stained) (C&D- X 100; H&E stained)

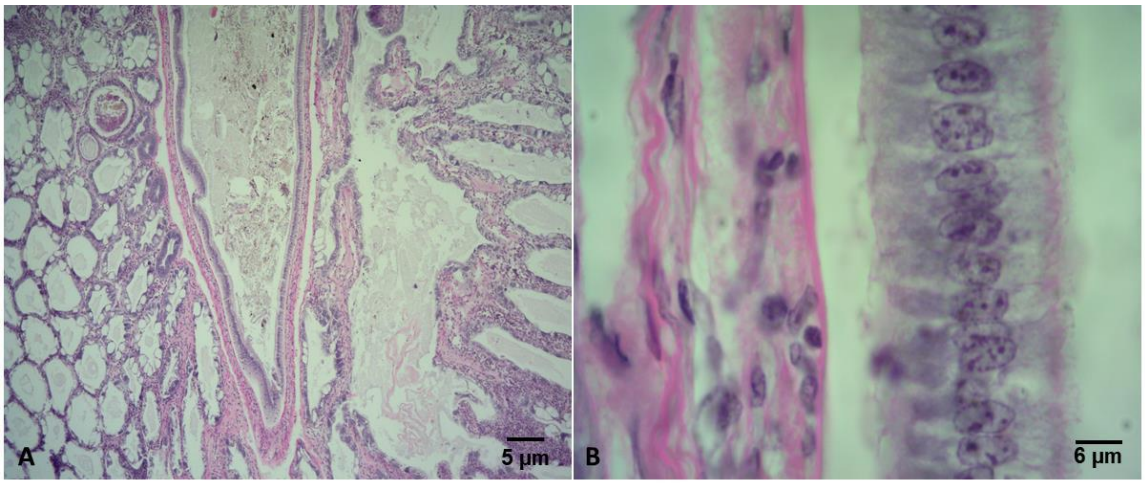

Plate 14. Normal gut histology. **(A)** Histological section showing normal intact epithelial lining. Note the moderate necrosis observed in the hepatopancreas and the hepatopancreatic duct connecting the HP to anterior midgut (x 40; H&E stained). **(B)** Histological section (Enlarged view) showing normal midgut epithelial lining and basement membrane (x 1000; H&E stained).

In the case of animals showing co-infection with EHP and bacteria, discernible pathological changes could be observed. This included severe necrosis marked by complete degeneration of the gut epithelium (Plate15 & 16). In these samples, the hepatopancreatic duct connecting the mid gut also showed severe necrosis (Plate 15). In some cases, the necrosis was severe and complete lysis of epithelial layer of midgut and adjoining hepatopancreas was observed (Plate 16).

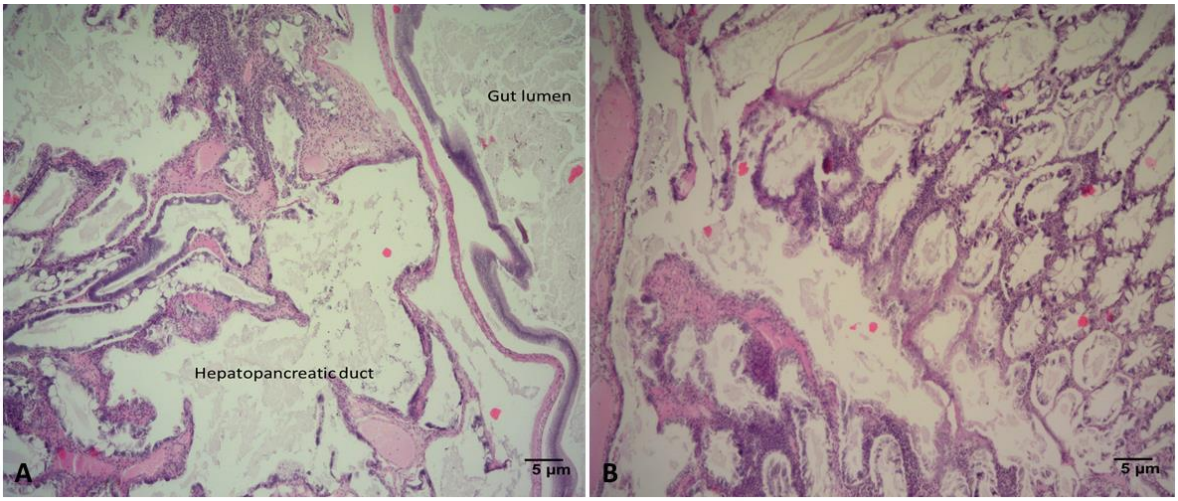

Plate 15. Necrosis of gut epithelium. **(A)** Histological section of hepatopancreas and gut showing the necrotized tubules & duct and necrotized gut epithelium (x 100; H&E stained). **(B)** Histological section of hepatopancreas and gut showing the necrotized tubules and duct and necrotized gut epithelium (x 100; H&E stained).

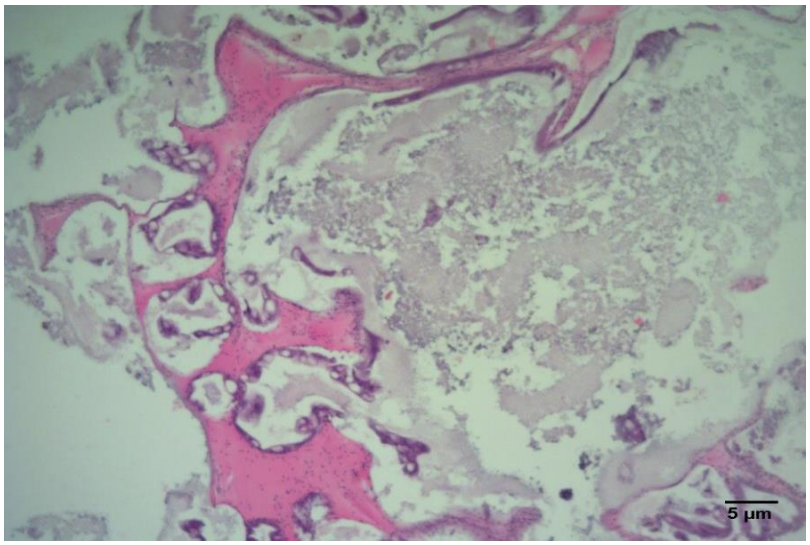

Plate 16. Histological section of gut showing complete degeneration of the gut epithelium and adjoining hepatopancreatic tubules (x 100; H&E stained)

4.2 PCR analysis

Samples of DNA extracted from hepatopancreas and gut were subjected to PCR amplification for the detection of EHP, WSSV, IHHNV, HPV, MBV, AHPND and NHP. Of the pathogens tested, PCR amplification could be detected only for EHP. The PCR was carried out using a set of EHP-specific primers (SWP F1R1 & SWP F2R2) yielded 148 bp product after second step in the nested PCR.

Out of 30 animals collected from inland saline water (Haryana), 6 animals were found EHP-positive by nested-PCR. Of the 30 animals collected from brackishwater ponds only 15 animals were subjected to PCR analysis. Nine out of 15 animals showed positive amplification for EHP in the nested PCR. Interestingly, none of the samples showed positive amplification in the first-step PCR. A representative gel picture showing the amplified PCR products of EHP is given in Plate 17 and the summary of the results of PCR analysis carried out during the present study is given in Table 12.

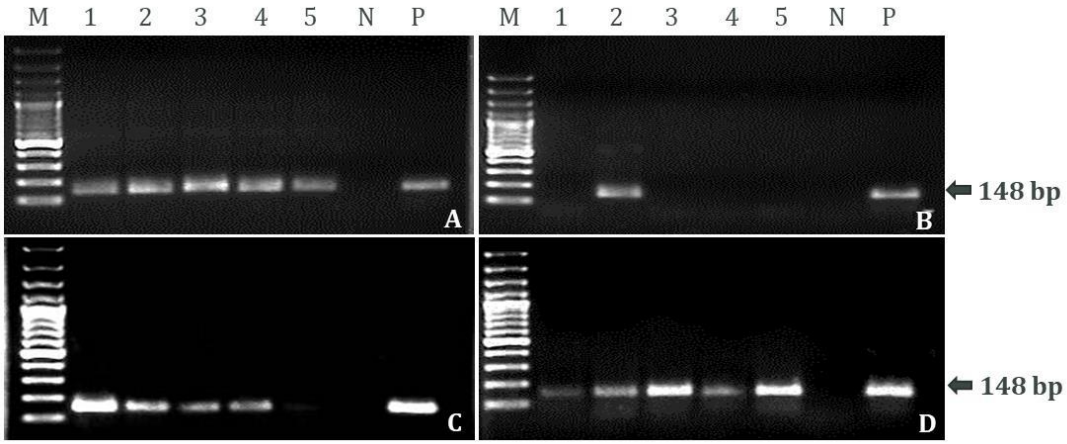

Plate 17. Agarose gel electrophoresis of second step PCR products of nested PCR carried out using a set of EHP-specific primers (SWP F1R1 & SWP F2R2). Panels A & B indicate the samples from Haryana and panels C & D indicate the samples from Maharashtra. M- 100 bp plus molecular weight marker; 1-5- sample number; N- negative control; P- positive control.

Table 12. Summary of the results of PCR analysis

Pathogens tested	No. of animals collected	Maharashtra (Brackishwater)			Haryana (Inland saline water)		
		No. of animals tested	No. of PCR positive	Prevalence	No. of animals tested	No. of PCR positive	Prevalence
EHP	60*	15	9	60.0%	30	6	20.0%
IHHNV		15	-	-	30	-	-
WSSV		15	-	-	30	-	-
MBV		15	-	-	30	-	-
HPV		15	-	-	30	-	-
NHP		15	-	-	30	-	-
Vp_{AHPND}		15	-	-	30	-	-

** Thirty animals each were collected from Maharashtra and Haryana, respectively, of which only 15 animals from Maharashtra were PCR tested*

DISCUSSION